EXPERIMENTAL OPTIMIZATION OF HYDRAULIC MINI-TURBINES

Bernardo Farrero

Dissertation presented to the **Escola Superior de Tecnologia e Gestão - Instituto Politécnico de Bragança – Portugal**, to obtain the Master degree in Industrial Engineering - Mechanical Engineering, in the joint double diplomacy with the **Faculdad Regional Cordoba - Universidad Tecnológica Nacional - Argentina**.

Supervisors

Professor Sergio Manuel de Sousa Rosa (PhD)

Professor Fabian Agostini (PhD)

September 2022

EXPERIMENTAL OPTIMIZATION OF HYDRAULIC MINI-TURBINES

Bernardo Farrero

Dissertation presented to the **Escola Superior de Tecnologia e Gestão - Instituto Politécnico de Bragança – Portugal**, to obtain the Master degree in Industrial Engineering - Mechanical Engineering, in the joint double diplomacy with the **Faculdad Regional Cordoba - Universidad Tecnológica Nacional - Argentina**.

Supervisors

Professor Sergio Manuel de Sousa Rosa (PhD)

Professor Fabian Agostini (PhD)

September 2022

ABSTRACT

The use of technologies to obtain energy from renewable sources has developed extensively over time and some of them are consolidated, such as hydroelectric power plants and wind turbines.

On the other hand, there are still areas with a lot to increase and that has great potential. One of the energy sources is water. Hydroelectric is one of the main renewable generators of. However, there are still areas of technology with a low degree of maturity, such as energy from marine currents and the generation of electricity through mini-turbines in river flows.

In this sense, this work presents a method based on the Blade Element Moment Theory to calculate the blade elements of a horizontal axis mini turbine, vary its geometry and allow a better e of power.

After the creation of a code in the Excel software and using parameters already calculated in another work, five different propellers were developed. Through the results obtained through the code, the modelling was carried out in the SolidWorks software. Then, it was possible to do the optimization of the chord of the blades, 3D print prototypes, and make the experimental comparison.

The results of the experimental tests carried out showed the influence of the tip speed ratio factor (λ) on the performance of an axial propeller and. These results are consistent with the literature that recommend values of λ based on the number of blades that make up a propeller. propeller. On the other hand, the importance of considering the number of blades that will make up a propeller when projecting the aerodynamic profile and how this affects its performance was demonstrated.

Keywords: Hydroelectric power. Turbines. Blade element. Tip speed ratio.

RESUMO

O uso de tecnologias que extraem energia de fontes renováveis tem se desenvolvido consideravelmente nos últimos anos, e algumas já se encontram bem implementadas, tais como hidroelétrica ou eólica. Por outro lado, ainda existem fontes renováveis com muito potencial para se desenvolverem, como é o caso da energia renovável obtida por correntes de água, cujas tecnologias existentes têm ainda um baixo grau de maturidade, tais como energia obtida por correntes marítimas ou em rios, com a geração de eletricidade através de mini turbinas.

Nesse sentido, este trabalho apresenta um método baseado na Teoria do Momento dos Elementos de Lâmina para calcular os elementos de lâmina de uma mini turbina de eixo horizontal, para assim variar a sua geometria, permitindo obter maior potência.

Após a criação do código no Excel e a utilização de parâmetros já calculados em outro trabalho anterior, foram desenvolvidas cinco hélices diferentes. Através dos resultados obtidos nos códigos, a modelagem foi realizada no SolidWorks, levando em consideração a otimização da corda das pás, possibilitando a impressão 3D e depois a comparação experimental.

Os resultados dos testes experimentais mostram a influência da relação velocidade de ponta (λ) no desempenho de uma hélice axial e como esses resultados estão de acordo com a literatura que recomendam valores de λ com base no número de pás que compõem uma hélice. Por outro lado, foi demonstrada a importância de se levar em conta o número de pás que irão compor uma hélice ao projetar o perfil aerodinâmico e como isso afeta seu desempenho.

Keywords: Energia hidroeléctrica. Turbinas. Elemento de Pá. Relação velocidade de ponta.

INDEX

LIST OF FIGURES

LIST OF TABLES

LIST OF SYMBOLS

C_{2u}	Absolute tangential velocity of the output fluid.
ω	Angular velocity.
P_S	Available power.
a	Axial interference coefficient.
$C_{P\ Betz}$	Betz power coefficient.
R	Blade radius.
C	Chord.
Z	Confidence level.
A	Cross section of the turbine.
Q_d	Design expense.
H_d	Design loading.
D_i	Diameter of the cube.
C_D	Drag coefficient.
F_D	Drag force.
$C_{P\ drag}$	Drag power coefficient.
μ	Dynamic viscosity.
dr	Element differential.
Y	Energy exchanged.
φ	Flow angle.
Q	Flow.
U	Fluid velocity.
η_g	Generator efficiency.
g	Gravity.
Δh	Height of water column.
P_h	Hydraulic power.
$C_{P\ ideal}$	Ideal power coefficient.
C_L	Lift coefficient.
F_L	Lift force.
λ_r	Local tip speed ratio.

$\dot{m}$	Mass flow.
C_N	Normal coefficient.
B	Numbers of blades.
N_{opt}	Optimal sampling size.
β	Pitch angle.
C_P	Power coefficient.
d_P	Power differential.
P_t	Power of a turbine.
η_B	Power reduction factor.
P	Power.
d	Precision.
q	Probability of failure.
p	Probability of success.
r	Radius to the element.
V	Relative speed.
Re	Reynolds.
D_e	Rotor diameter.
σ	Solidity.
ρ	Specific mass.
V_w	Speed as a function of radius.
K	Storage factor.
C_T	Tangential coefficient.
U_1	Tangential input velocity.
b	Tangential interference coefficient.
U_2	Tangential output speed.
C_{1u}	The absolute tangential velocity of the input fluid.
α	The angle of attack.
λ	Tip speed ratio.
dt	Torque differential.
T	Torque.
η_t	Turbine efficiency.

F	Unique factor of losses.
γ	Volumetric weight.

LIST OF EQUATIONS

1. INTRODUCTION

The world's main energy source continues to be fossil fuels and their derivatives. These, in general, have large amounts of pollutants that are discarded in nature; In addition, its gases harm the nature, as it retains heat (Greenhouse Gases or GHG). Of global GHG emissions, 35% corresponds to gases generated by the energy sector. Fossil fuels are the ones that emit the most carbon s per unit of energy supplied.

Mitigation measures will need to be directed to improve energy efficiency, which is why national governments around the world have putting place new regulations to able to expand renewable energy sources. One of these sources of energy is through water, being the case of hydroelectric one of the main generating matrices of electricity by renewable energies. However, it still has areas of technology with a low degree of maturity, such as the energy of marine currents and the generation of electricity through mini turbines in river flows.

The use of mini electric turbines has great advantages, not only contributing to the depollution of the environment, but also energy diversification and the possibility of social development in communities that are not connected to the electricity distribution grids.

The mini hydraulic power plants are simple installations. They are easy to install and have low maintenance costs. They require few components: Turbine group - generator - regulator system. They are generally connected to a group of batteries.

1.1 OBJECTIVE

The objectives of this work, in addition to disseminating as much as possible the technology of mini turbines for the generation of electrical energy in a sustainable way, is to experimentally compare the performance of propellers with different parameters.

In this way, a series of objectives were proposed to be met:

1. Following Souza's recommendation [1], the first objective of the present work is to create a code to be able to obtain the parameters of a 3-blade propeller without taking into account the interference factors. (Null interference factors)

2. With the code obtained, the second objective is to generate 3 propellers with different values of tip speed ratio (λ) (λ=1, λ=2, and λ=3) and then make compare them.

3. With the parameters obtained, the third objective is to create the design of the propeller through SolidWorks 2021 software.

4. Then, 3D prints the propellers for further experimental tests.

5. Corroborate the influence of the tip speed ratio parameter (λ) and compare with the experimental table.
6. Compare the results of "optimized" and "non optimized" turbine of 10 blades exposed by Souza [1], by reducing the blade numbers (B) (from 10 to 3) without modifying the chord values or construction parameters.

2. STATE OF THE ART

2.1 MACHINE

Machine is an energy transformer. It absorbs one kind of energy and returns another type of energy (or energy of the same class, but transformed).

Thus, while a fan absorbs mechanical energy from rotation on its axis and returns it in the form of pressure and/or dynamic energy to the fluid, an electrical transformer raises the voltage while maintaining the same type of electrical energy.

2.2 FLUID MACHINE

Fluid machines are those in which the fluid supplies energy absorbed by the machine (hydraulic turbine) or the fluid is a receiver to which the machine returns the absorbed mechanical energy (fluid pump).

We can adopt the principle of operation criterion to be able to classify fluid machines into positive displacement machines and turbo machines. Other classification criteria can be the compressibility of the fluid and the direction of energy transmission. Due to the interest of this present work, we will only expand on the classification of turbomachines.

2.3 TURBOMACHINES

Turbomachines are those fluid machines in which the exchange of energy is due to the variation of the kinetic moment of the fluid when passing through the ducts of an organ that moves with rotational movement, equipped with blades or vanes that are called the rotors

A popularized definition concerning the previous one for turbomachines where these machines are defined with absolute precision is:

"TURBOMACHINE IS A FLUID MACHINE WHOSE OPERATION IS BASED ON THE EULER EQUATION OR FUNDAMENTAL EQUATION OF TURBOMACHINES"

This equation expresses the energy exchanged between the rotor and the fluid:

$$Y = u_1 c_{1u} - u_2 c_{2u} \left[\frac{J}{kg}\right] \quad [1]$$

Where:

- Y: Energy exchanged.
- u_1: Tangential input velocity.
- c_{1u}: Absolute fluid velocity. Input tangential component.
- u_2: Tangential output speed.
- c_{2u}: Absolute fluid velocity. Output tangential component.

According to the compressibility of the fluid during the exchange of energy we can make a new division within the classification of the turbomachines, although all real fluid is compressible, in practical terms we can say that the variation of the specific volume in liquids such as water, for example, is so small that it can be disregarded. Thus, we arrive at a new definition of hydraulic turbomachines which will be important for this work:

"TURBOMACHINE IS THAT FLUID MACHINE WHOSE OPERATION IS BASED ON THE EULER EQUATION OR FUNDAMENTAL EQUATION OF TURBOMACHINES, AND WHOSE STUDY AND DESIGN IS DONE WITHOUT TAKING INTO ACCOUNT THE VARIATION OF THE SPECIFIC VOLUME (DENSITY) OF THE FLUID THROUGH THE PASSAGE OF THIS ENVELOPE MACHINE".

2.4 HYDRAULIC TURBOMACHINES

As already defined in the previous section, it is a turbomachine, and that during the passage of the fluid on it there will be no variation in density. So, we can classify the types of hydraulic turbomachines according to the function they perform:

Motor, collect the energy given by the fluid that crosses them, and transforms them into mechanics, being able to be of the Dynamic or Static type.

Generative, increase the energy of the fluid that passes through them in the form of potential or kinetics; the mechanical energy consumed is supplied by a motor.

Reversible, they are both motor and generative, the most important is the turbine-pump groups and the bulb groups.

Coupling, are a combination of motor machines and generative, that is, a coupling (pump-turbine) in a closed circuit.

Within the classification of hydraulic motor turbomachines, there are hydraulic turbines, which will be the object of study in this work. Having noted this, we will define and classify hydraulic turbines.

2.5 HYDRAULIC TURBINES

The potential energy of water can be transformed into kinetics if there is any height difference due to the unevenness. Hydraulic turbines take advantage of the speed carried by the water to be able to transform that energy into useful energy, either mechanical or electrical.

An elementary turbomachine consists of a series of fixed blades (distributor), a series of moving blades (impeller, wheel, rotor), and finally a diffuser.

The distributor and diffuser are part of the stator of the machines, that is, they are fixed organs; these can be omitted in certain machines.

The distributor is a fixed organ whose objective is to redirect the water from the entrance section of the machine to the entrance of the impeller, either by redistributing the whole of it (total admission) or a part (partial admission). This organ is also capable of transforming energy from pressure into speed.

The impeller is the essential element of the turbine. It is equipped with blades in which the exchange of energy between the water and the machine takes place. In this organ, depending on whether or not the pressure varies during the flow of the fluid two large groups of hydraulic turbines are defined: action turbines and reaction turbines.

Another important classification within hydraulic turbines is according to the direction of water inlet into the turbines:

- Axial.
- Radial.
- Mixed.
- Tangential.

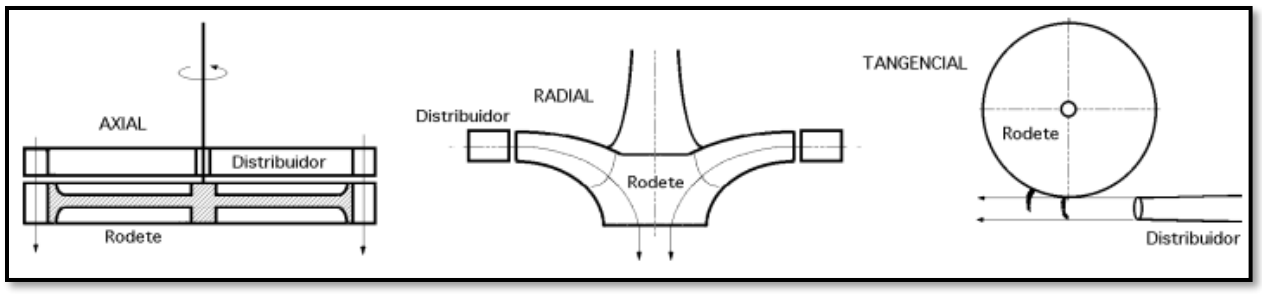

Figure 1. Types of hydraulic turbines

The axial ones are those that the fluid enters parallel to the axis.

The radials, (also known as Francis turbine) are those where water enters perpendicular to the axis.

The mixed, a combination of axial and radial.

The tangential, (or Pelton turbine) water enters laterally or tangentially against the blades.

2.5.1 Action turbines

In action turbines the water leaves the distributor at atmospheric pressure, and reaches the impeller with the same pressure. In these turbines, all the potential energy of the enthalpic jump is transmitted to the impeller in the form of kinetic energy.

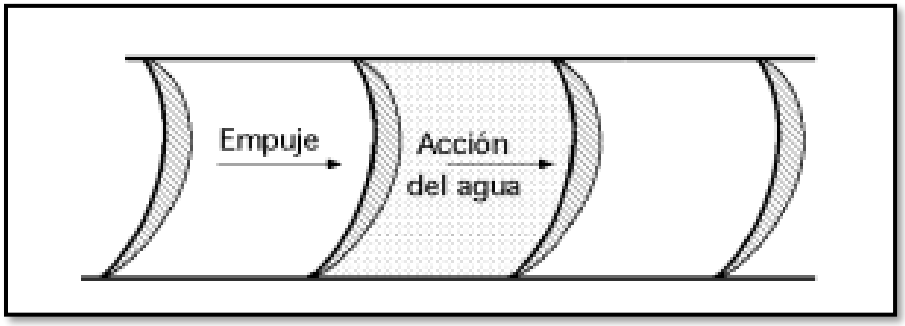

Figure 2. Action turbines.

Some examples of the most used in practice are:

- Zuppinger turbine.

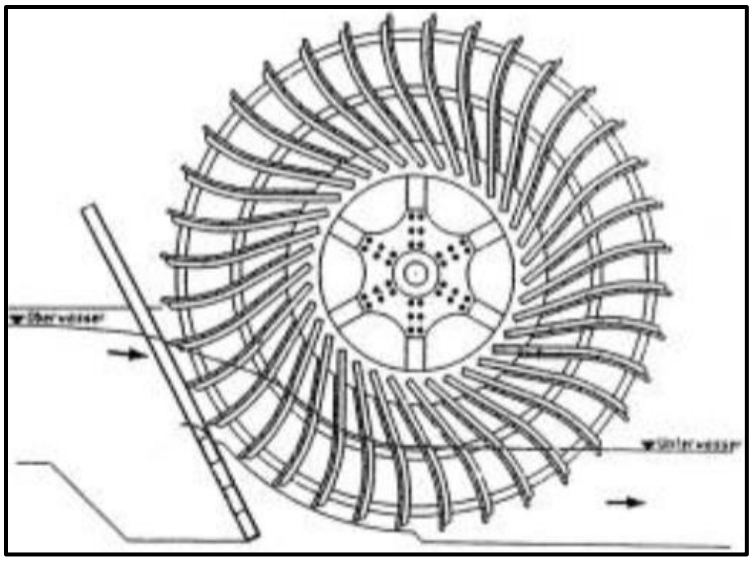

Figure 3. Zuppinger turbine.

- Pelton turbine.

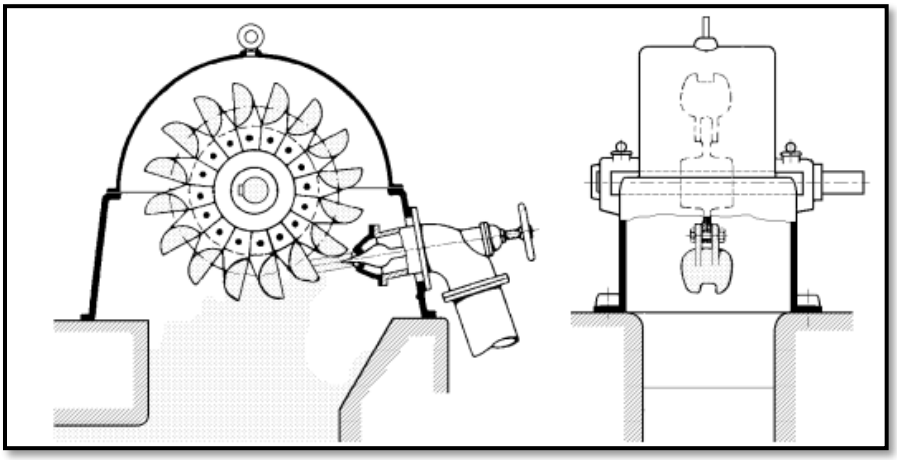

Figure 4. Pelton's turbine.

- Michel turbine.

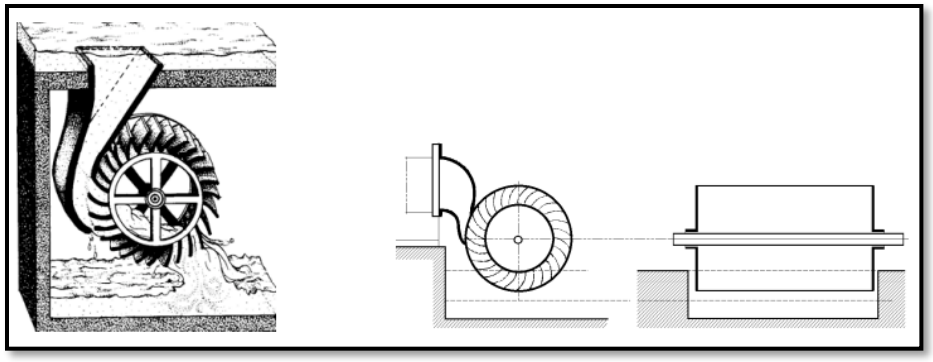

Figure 5. Michel turbine.

- Schwamkrug turbine.

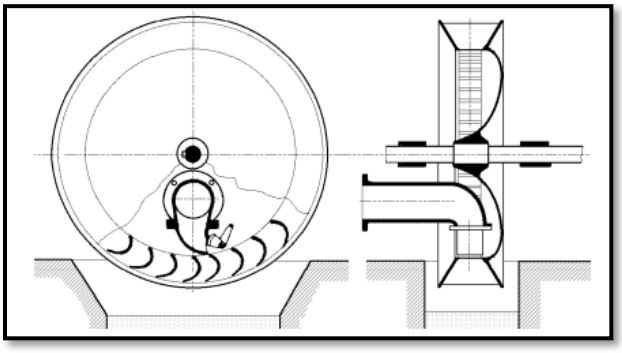

Figure 6. Schwamkrug turbine.

- Girad turbine.

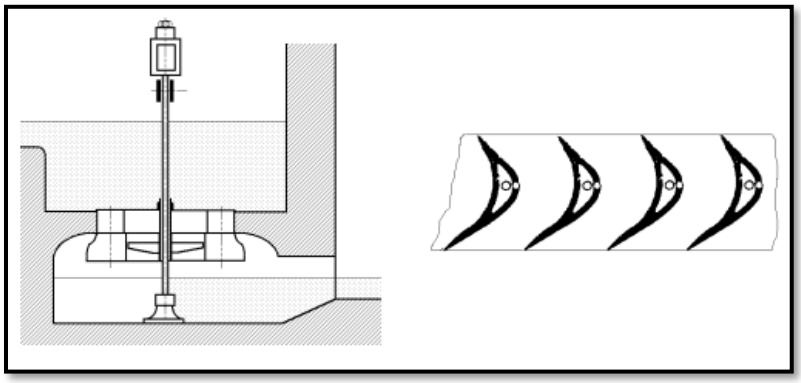

Figure7. Girad turbine.

2.5.2 Reaction turbines

In reaction turbines the water leaves the distributor with a certain pressure that decreases as the water passes through the impeller blades. So that, at the outlet, the pressure can be zero or even negative. In these machines the water circulates under pressure in the distributor and in the impeller. Therefore, the potential energy of the enthalpic jump is transformed one part into kinetic energy and the other into pressure energy.

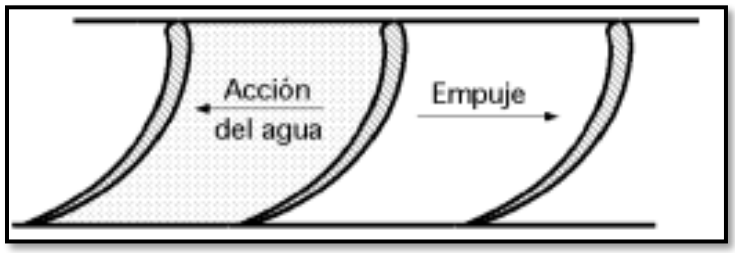

Figure 8. Reaction turbine.

Some examples of most used in practice are:

- Fourneyron turbine (radial).

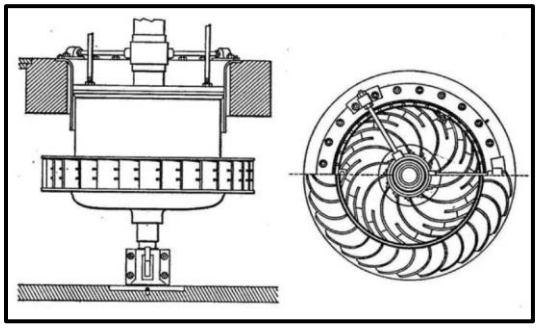

Figure 9. Fourneyron turbine.

- Francis turbine (radial).

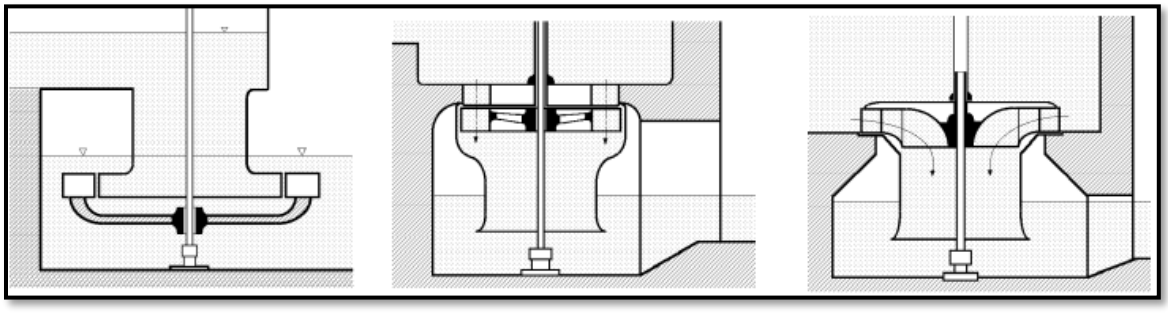

Figure 10. Francis turbine.

- Heuschel-Jonval turbine (axial).

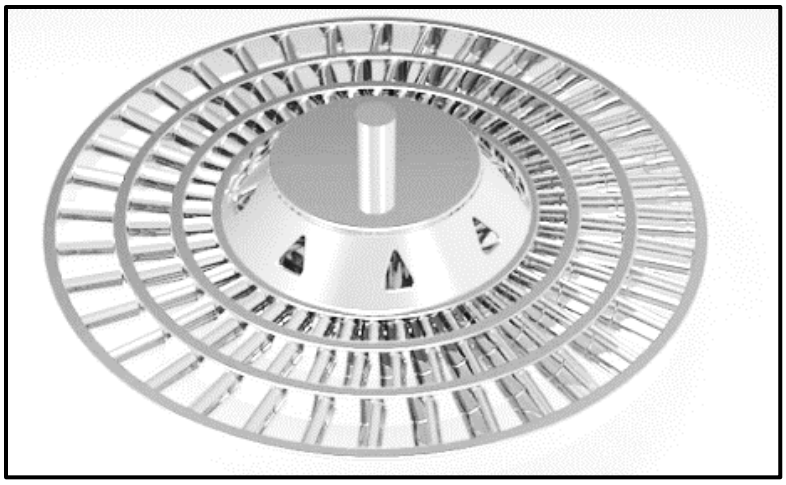

Figure 11. Heuschel-Jonval turbine.

- Kaplan turbine (axial).

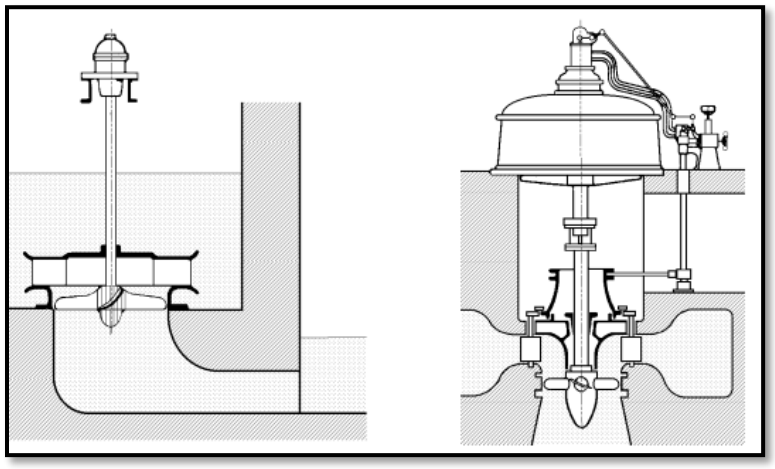

Figure 12. Kaplan turbine.

2.6 CRITERIA FOR TURBINE SELECTION

In order to carry out the selection of the most suitable turbine for a project it is first necessary to determine the capacity to be installed in a hydroelectric exploitation, once this value has been obtained, the calculation of the power P_t, load H_d and expense can be continued Q_d.

Where the turbine power is:

$$P_t = \frac{installed\ capacity * K}{N°\ units * \eta_g} \quad [2]$$

Where:

- P_t= turbine power [kW].

- K= factor that depends on storage characteristics (0,85 -1,30).
- η_g= generator efficiency (0,98).

Being that if the power is expressed in kW:

$$Q_d = \frac{P_t}{\eta_t * H_d * \gamma} \quad [3]$$

Where:

- Q_d= design expense [m^3/s].
- P_t= power [kW].
- η_t= turbine efficiency [%].
- H_d= design load [m].
- γ= volumetric weight of water [kgf/m^3].

Where H_d is the design load of the turbine in meters and can be between $H_{min}\ and\ H_{max}$. It is convenient that this value is H_d close to the most frequent net load.

The Figure shows a diagram representing the recommended regions for different types of hydraulic turbines depending on the parameters H_d and Q_d.

It can also be observed that with the design expense Q_d and load H_d it is possible to have a pre-selection of the turbine type between Pelton, Francis and Kaplan with a power range of the order of 1 to 600 [MW]. This pre-selection allows to choose the appropriate regression equations for the type of turbine. The range of values allows to verify that the appropriate turbine is selected. And it will be verified with the synchronous rotation speed N', the specific speed Ns and the dimensions of the impeller, especially in the Francis type specified below.

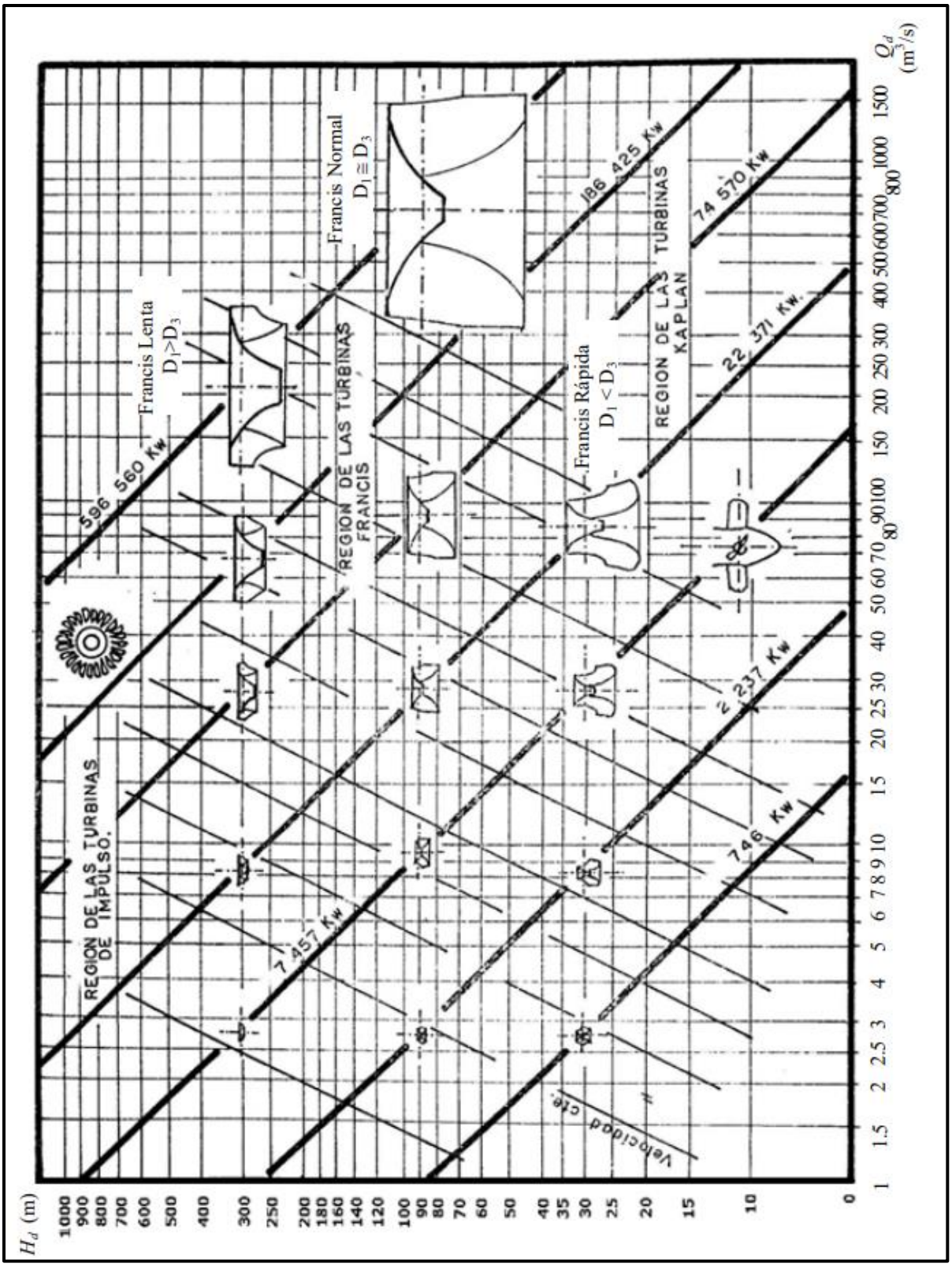

Figure 13. Selection of pumps.

In this case, Francis turbines can be of three types:

- SLOW $D_1 > D_3$.
- NORMAL $D_1 \cong D_3$.
- FAST $D_1 < D_3$.

Being D_1 and D_3 the diameters of the spiral chamber.

2.7 MINI TURBINES

Uses of mini turbines for mini hydropower systems can be made on any occasion where an energy supply is necessary. Only the presence of a watercourse and a small potential jump of a few meters is needed. In these cases, mini plant has a reduced impact being that it does not modify the water flows that can be vital for some isolated areas and the local fauna. Mini-hydraulics is a term by which the UNDO (United Nations Industrial Development Organization) refers to hydroelectric power plants that do not exceed 10 [MW].

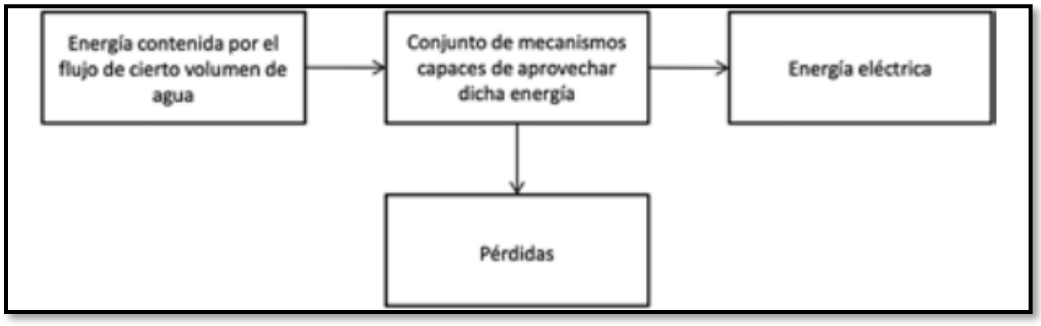

Figure 14. Electric power generation process.

Turbinas de Impulso	
Mini turbinas Pelton	Son turbinas de acción donde uno o más chorros inciden en una rueda que posee en su periferia un gran número de álabes La turbina Pelton es un tipo de turbina de impulso y es la más eficiente en aplicaciones donde se cuenta con un gran desnivel de agua.
Turbinas de flujo cruzado (Banki-Michell, u Ossberger)	Para una amplia gama de caudales entre 20 l/s y 10 m^3/s y alturas entre 1 y 200 metros. El agua entra en la turbina, dirigida por uno o más paletas de guía situada en una pieza de transición aguas arriba. El Flujo sale y cruza el centro de la turbina. Su eficiencia es menor que las turbinas convencionales, pero responde a una amplia gama de caudales y de alturas.
Turgo	La turbina Turgo es una turbina de impulso diseñada para saltos de desnivel medio. Fue desarrollada por la compañía Gilkes en 1919 a partir de una modificación de la turbina Pelton. Se recomiendan para sitios con importantes variaciones de flujo de agua y aguas turbias
Turbinas de Reacción	
Mini turbinas Francis	Son turbinas de reacción válida para centrales de tamaño medio, con potencia aproximada de 100 kW. La ventaja de esta máquina consiste en el aprovechamiento de todo el salto disponible, hasta el canal de desagüe. La construcción es compleja lo que hace problemática la instalación de estas turbinas en las centrales pequeñas
Kaplan y turbinas de hélice	Son turbinas de reacción de flujo axial. Se emplean en saltos de pequeña altura. Las palas o álabes de la turbina son impulsadas por agua a alta presión liberada por una compuerta. Las turbinas de hélice se caracterizan porque tanto los álabes del rodete como los del distribuidor son fijos. Sólo se utilizan cuando el caudal y el salto son prácticamente constantes
Bombas utilizadas como Turbinas	El uso de Bombas Centrífugas Standard como turbinas puede ofrecer una alternativa técnica y con ventajas económicas y pueden contribuir a una amplia aplicación en pequeñas centrales hidráulicas. Las bombas con sentido de rotación inverso, están siendo utilizadas como turbinas en aplicaciones industriales, y más recientemente en centrales para sitios aislados.

Figure 15. Classification of turbines.

As in the case of hydraulic turbines, in mini turbines we can also be divided into different types according to whether the expansion is obtained in the fixed or mobile elements, that is, impulse or reaction. Reyna [6] (Figure 15.)

Depending on the estimated characteristics of jump, flow, and the power needed, it is possible to obtain the most suitable type of mini turbine.

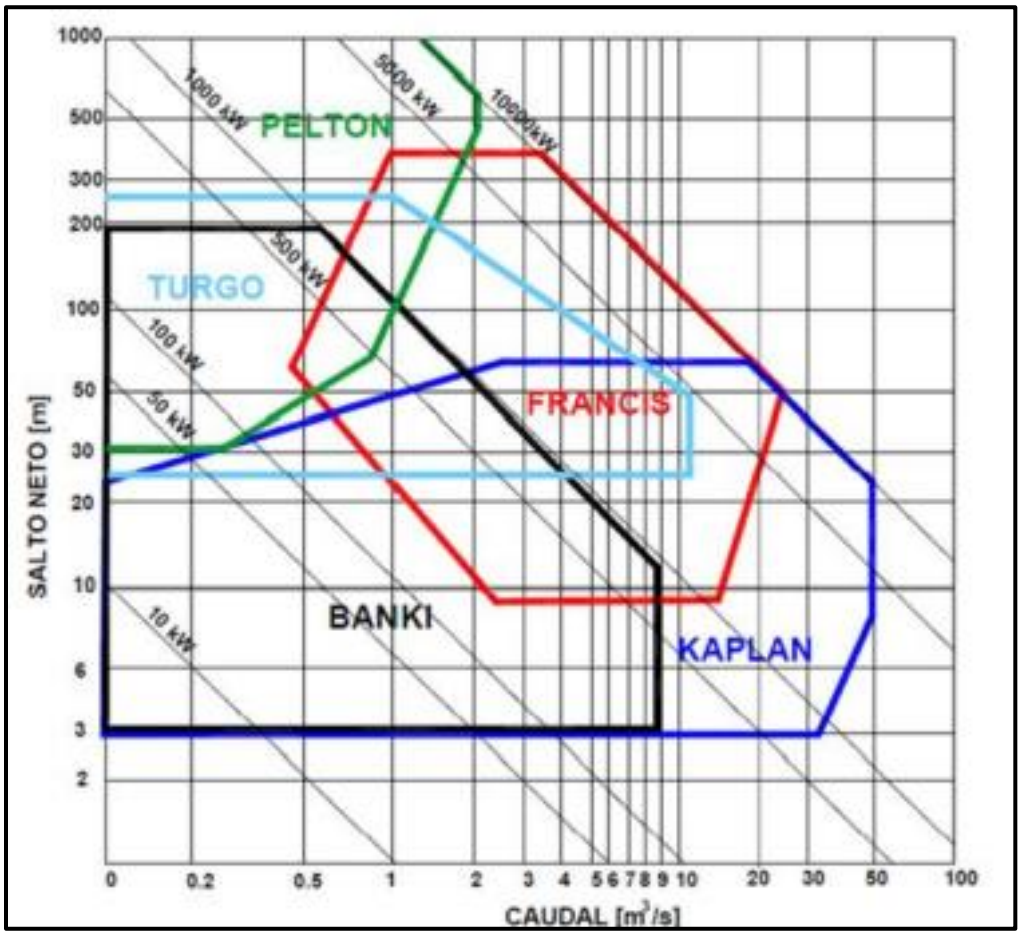

Figure 16. Turbine selection chart.

Next, a detailed description of the characteristics of each type of machine will be carried out.

2.7.1 Michel-Banki

The Michel-Banki turbine is a machine classified as an action, radial inlet, and transverse flow turbine. Used mainly for small hydroelectric exploitations, its main advantages are in its simple design and easy construction, which makes it attractive in the economic balance of a small-scale use (ITDG, 2009).

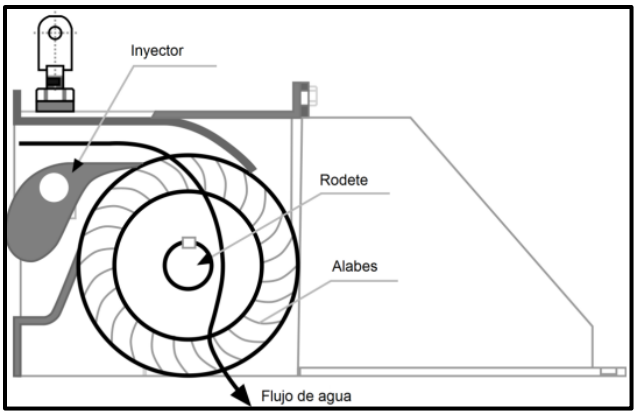

Figure 17. Michel-Banki turbine.

The main features of this machine are as follows:

- The rotational speed can be selected over a wide range.
- It can operate in wide flow and height ranges without appreciably changing its efficiency.
- The diameter of the turbine does not necessarily depend on the flow rate.
- An acceptable level of performance is achieved with small turbines.
- Flow rate and power can be regulated using an adjustable blade.
- Its construction is simple, being able to be manufactured in small workshops.

The transverse flow turbine is especially suitable for rivers with small flows, which usually carry very little water for several months. The energy of the water is transferred to the rotor in two stages, which also gives this machine the name of the double-acting turbine, and of which the first delivers an average of 70% of the total energy transferred and the second about 30% remaining. Finally, the water is returned by a discharge at atmospheric pressure (degree of reaction equal to zero)

2.7.2 Kaplan

The Kaplan micro turbine is a machine classified as a reaction, inlet and axial flow turbine. It is mainly used for small hydroelectric exploitations and also has the advantage of its simple design, which makes it attractive for small-scale use. This type of micro turbine are usually installed on the small leveling dams of rural areas. The mini-Kaplan, unlike an ordinary Kaplan turbine used in large hydroelectric, has the particularity of the absence of a peripheral spiral chamber and the set of mobile stators directors blades that direct the flow to the rotor of the machine, making the water a radial – axial path.

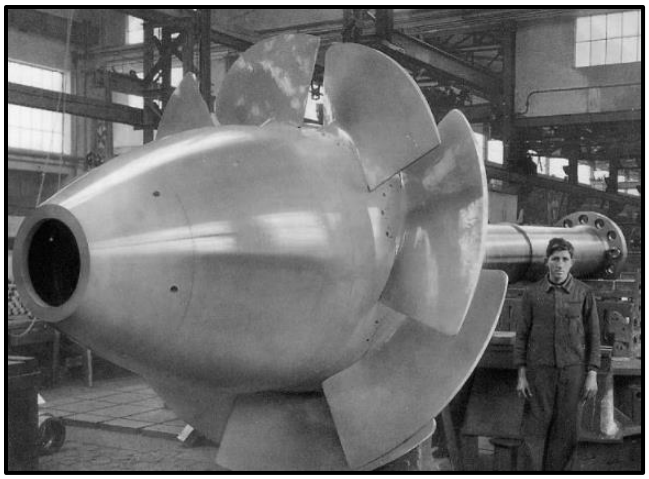

Figure 18. Axial-Kaplan turbine.

Its impeller is composed by a few blades, which give it the shape of a ship propeller. When these are fixed, it is called a propeller turbine, while if they are steerable, they are called Kaplan turbines. In both cases the turbines operate with a single direction of rotation; they are therefore irreversible turbines. Its main features are:

- Reduced dimensions.
- Relatively high speeds.
- High performance with variable load.
- Remarkable capacity for overloads.

The wing profile allows obtaining a useful action of the water on the blade in the movement that it has concerning it. The helical shape or warp is justified due of the fact that the relative velocity of the flow varies in direction and magnitude according to the radius It is supposed ω (angular velocity), absolute velocity in magnitude, and direction constant. In addition, a polished surface finish is required for the blades. The allowed roughness between the contact surface and the water depends on the flow rate.

The manufacture of the blades is the main drawback to achieve an economical equipment, because it requires precision casting. If only blades of constant thickness, flat or curved are used, lower coefficients of support and greater resistance are obtained. As a consequence, the efficiency would be lower, in addition to not taking full advantage of the exchange of energy by the fluid when it affects the blades. An example of efficiencies is in the article written by Espinoza (1991), where the axial turbine without using aerodynamic blades obtained an efficiency value of 40%.

2.7.3 Turgo

The Turgo Turbine is an impulse hydraulic turbine designed for medium jumps. It is a turbomachine engine of action, free jet, radial flow, used mostly for small hydroelectric. Their main advantage is in their simple design and easy construction, which makes them very attractive

in the economic balance of a small-scale use. It was designed by Eric Crewdson, managing director of the company "Gilbert Gilkes & Gordon Ltd", based in Kendal, United Kingdom; in 1919, from a series of modifications of the Pelton Turbine.

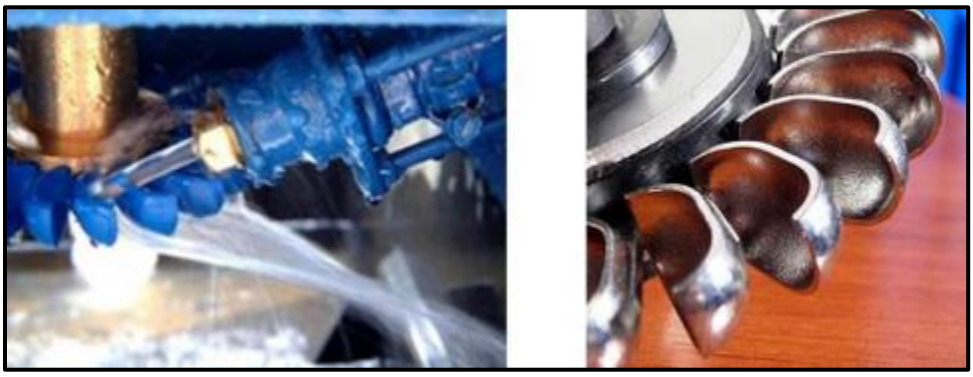

Figure 19. Turgo turbine.

The distributor of the Turgo turbine basically consists of an injector of the Pelton type (it consists essentially of a nozzle and a needle valve) that projects a jet of water inclined with respect to the axis of the Impeller, at an angle of 15º to 22.5º. The impeller resembles a Pelton half impeller, as if it were divided by a plane that passes through the edges of the spoons and is perpendicular to the axis. This turbine can be mounted with horizontal or vertical axis and has several advantages over the Francis and Pelton turbines in certain applications:

1) The impeller is cheaper to manufacture than that of a Pelton.

2) It isn't needed an airtight housing like the Francis.

3) For the same power, it has half the diameter which leads for equal peripheral speed, a higher angular speed. Then, it facilitates its direct coupling to the generator. As a consequence, it doesn't require the speed multiplier (what reduces the price of the group and decreases its vulnerability).

4) It can handle a greater flow of water than the Pelton, because the water coming out does not interfere with the adjacent pallets.

5) The performance of the Turgo turbine is less sensitive to flow variations.

6) They operate in a field of unevenness in which the Francis and Pelton turbines overlap.

Although there are many large installations with Turgo turbines, these are used more in small hydraulic installations where low cost is important.

2.8 WATER ENERGY

The use of water resources as an energy source is a practice whose origin dates back several millennia. Today, it is still just so useful, especially for the generation of electric power.

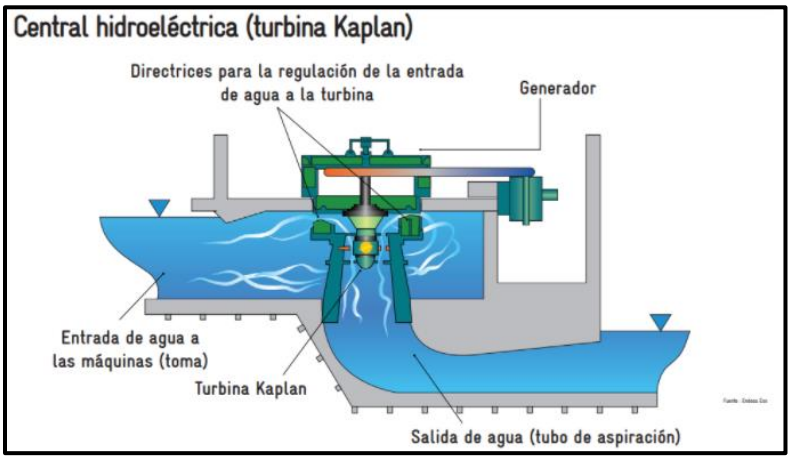

Figure 20. Hydroelectric power plant with Kaplan turbine.

For the generation of electricity, small hydroelectric plants use the movement of water, for example, in rivers, natural and artificial canals. The water, with its available hydraulic power, passes through a turbine which transforms it into mechanical power. It is then transformed into electrical power through a generator. From there, it goes to the transformers and then begins its journey to the centers of consumption.

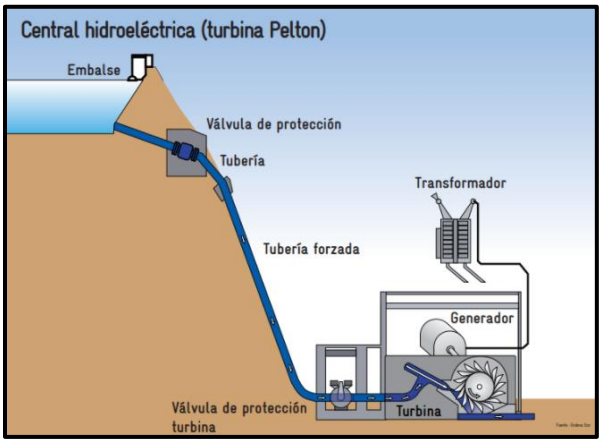

Figure 21. Hydroelectric power plant with Pelton turbine.

2.9 CURRENT PROJECTS

2.9.1 The Dominican Republic

In the Dominican Republic, non-conventional renewable energies (NCRE) are hydroelectric plants whose maximum power does not exceed 5 MW.

Table 1. Plants in the Dominican Republic.

Plants	Power [MW]
Aniana Vargas 1	0,3
Aniana Vargas 2	0,3
Baiguaque 1	0,6
Baiguaque 2	0,6
El salto	0,7
Los anones	0,1
Los toros 1	4,9
Los toros 2	4,9
Magueyal 1	1,5
Magueyal 2	1,5
Nizao Najayo	0,3
Rosa Julia de la Cruz	0,9
Brazo derecho	2,9
Contra embalse Monción 1	1,6
Contra embalse Monción 2	1,6
Domingo Rodriguez 1	2
Domingo Rodriguez 2	2
Las barías	0,9
Otras	1,8
Total	29,4

At the end of 2018, small hydroelectric plants contributed around 30 MW, which represents about 0.7% of the installed capacity in the country. Some of these micro hydroelectric plants (about 7%) are used in small towns where the energy generated is immediately used, without the plant being connected to the National Interconnected Electric System.

2.9.2 Spain

Spain is a country that has a long tradition in the area of hydropower. From the mid-nineteenth and early twentieth centuries the foundations for the generation of electricity in rural areas were forged with small local power plants. The technological development of high voltage lines and associated equipment for the transport of electricity over long distances, as well as the development of new energy transformation technologies based on fossil fuels in the mid-twentieth century, was displacing the mini-plants until they were abandoned. It was in the aftermath of the energy crisis of 1973 and 1979 that the need to diversify the primary energy sources used was highlighted. From here, the important role played by small-power hydroelectric power plants in the energy production system as a whole began to be assessed again. Due also to the environmental problems currently facing the whole planet, mini-plants, whether newly built or rehabilitated, are considered one of the most reasonable and viable options.

Table 2. Plants in Spain.

Plants	Power [MW]
Central Huesna	0,9
Hurones	0,5
Murias	6,6
Central Purón	0,4
Virgen de las viñas	1,7
Selga de Órdas	0,45
Porma	18
Lanzahita	1,9
Xerta	18
Jerte	0,5
Portodemouros	9,8

Tambre III	8,4
El barco	3,2
Antella-Escalona	3,9
Molino de Suso	3,2
Berberine Central	2,3
Total	79,75

2.9.3 Condor Mini Hydroelectric Power Plant

The Hydroelectric Exploitation of Condor is located in the Thunder River, composed of an 8 m high dam, inlet, sandblaster, pressure pipe, powerhouse with 2 Francis turbines, restitution, two substations, 23 km of transmission line, service road and access road. The main characteristics are: installed capacity of 5.5 MW, design flow of 6.0 m³/s, useful drop of 106 m and annual generation estimated at 18.5 GWh.

The Project consists of the Review of Basic Engineering and Detailed Engineering and includes Hydrological Studies, Energy Analysis, Geological and Geotechnical Studies, Hydraulic Axis Modeling, Structures Project, Analysis of transient regimes and protection devices, Electrical and Electromechanical Equipment Project, Electrical Installations Project, Substation and Transmission Line.

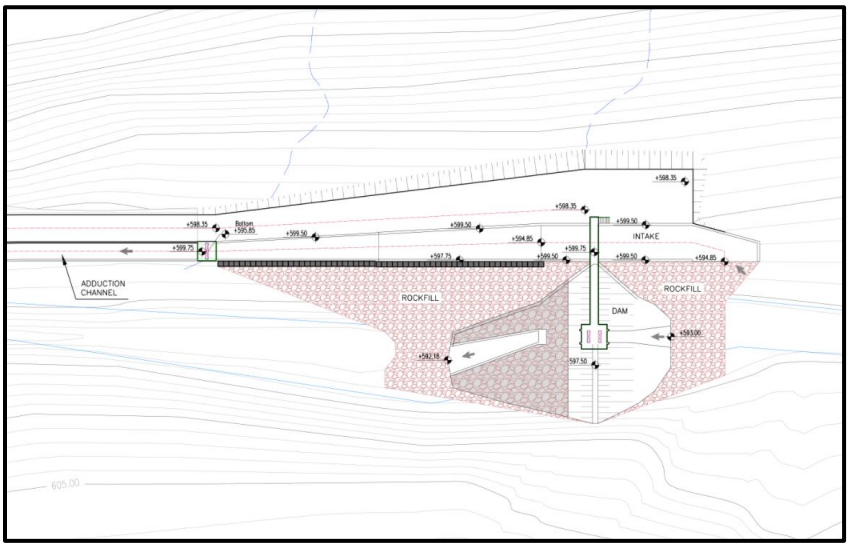

Figure 22. Mini central of the Condor.

3. METHODOLOGY

3.1 BLADE ELEMENT THEORY

This theory consists of the analysis of the rotor blades in such a way that they are divided into small length differentials (Figure 23). The two-dimensional geometric characteristics of the profile that forms its cross section are taken into account. Several authors agree with the following restrictions:

- The forces acting on the blade element will be the same in each element with the same profile, angle of attack or incidence, and effective speed.
- The operation of each blade element is not affected by the adjacent element. And the downforce of the entire blade is the sum of the force in each element.
- Knowing the characteristics of the profile, the forces and moments on the blades can be determined according to the interference factors a and b.

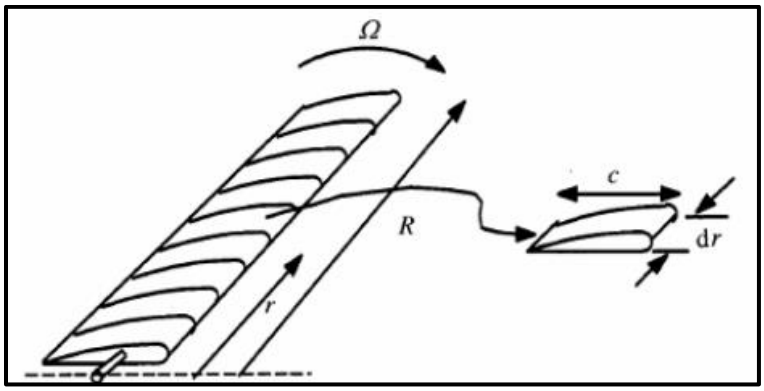

Figure 23. Division of the propeller in the theory of the blade element.

The rotor consists of (B) blades, radius (R), rotating at an angular speed (Ω) and the blade chord (c). (r) is the radius to the element.

3.1.1 Airfoil

The airfoil, or also aerofolio, corresponds to the cross section of a blade. There are several models, each with its own geometric peculiarities. On them, lifting and dragging forces are generated, in the direction perpendicular and parallel to the flow of fluid, respectively.

The aerial profiles have some nomenclatures that characterize them, extremely important to proceed with the equations.

The camber line, or skeleton, is the middle line between the top and bottom surface.

The leading edge and trailing edge, are located at the front and back ends, respectively, of the curvature line.

The chord is the distance in a straight line between the leading and exit edges.

The thickness, is the distance between the upper and lower surface, measured perpendicular to the chord.

The camber is the distance between the skeleton and the line of the chord.

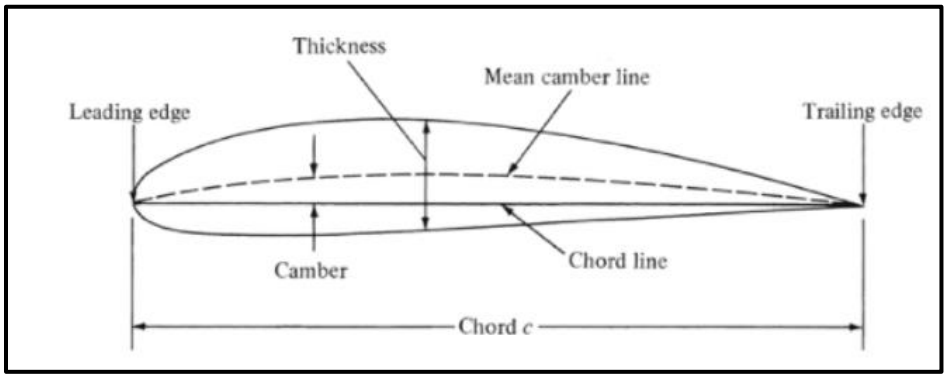

Figure 24. Airfoil nomenclature

The most commonly used airfoils in turbines and aviation are from the National Advisory Committee for Aeronautics (NACA). There are several series of NACA profile aerodynamic profiles and these can be found in the NACA database freely and free of charge with their respective graphics.

Among all the series, there are the NACA 4-digit series that are characterized as follows:

- 1st Digit: Value of the relative arrow in percentage (f/c).
- 2° Digit: coordinate of the maximum arrow, xm, (10cm/c).
- 3° and 4°Digits s: thickness relative in percentage. (thickness/c).

3.1.2 Aerodynamic forces

The fluid flow, as it passes through the rotor blades, generate a distribution of forces along the extension of the profile. These forces are known as *drag* force and lift *force*. The first one is oriented parallel to the airflow and the second is perpendicular to it. The magnitudes of these forces depend exclusively on the specific mass of the fluid, the velocity, dimensions of the surface, and the shape and orientation of the aerodynamic body.

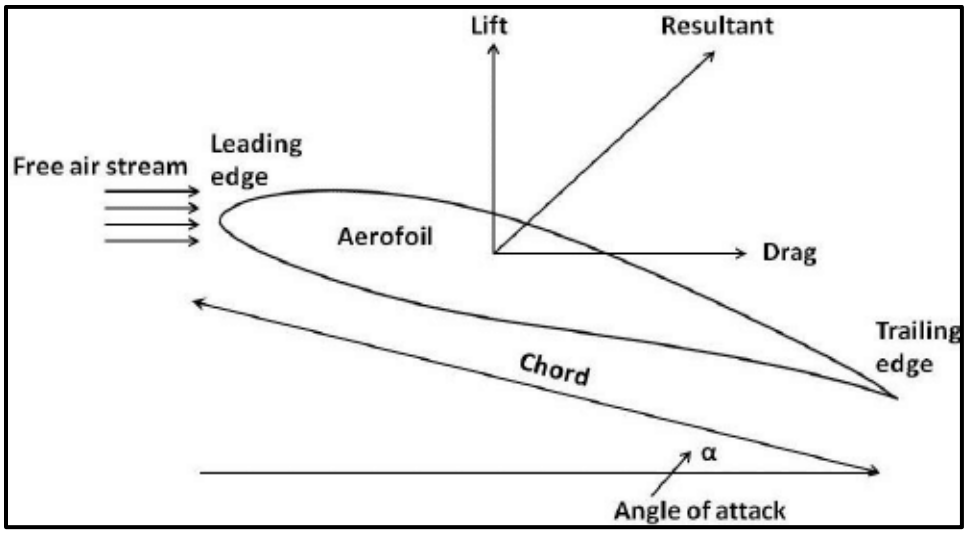

Figure 25. Unwrapped forces in the airfoil.

Under the influence of a flow, the airfoil makes it possible to increase the speed of the upper part, in this case, and a reduction in the lower part. With this, following Bernoulli's laws, it generates a decrease in pressure at the top. As a consequence, an area of high and low pressure is generated. It causes the lifting force perpendicular to the direction of the velocity of the free fluid. On the other hand, the passage of the fluid across the surface of the airfoil generates a drag force due to the friction of the fluid with the surface. This force is in a direction parallel to the free flow.

The use of dimensionless numbers to calculate the unwrapped forces is fundamental for the simplification of the problem, since the unfolding phenomena have complex dependence on geometric and flow parameters. These parameters are usually found by means of experimental tests and must be expanded for different conditions through interpolation.

It would be unfeasible to perform tests for all the different types of profiles and infinite velocity values that the fluid can assume. It would take a long time and unimaginable number of

tests. Then, instead of performing the tests, through dimensional analysis and similarity, it is possible to establish a relationship between the experimental and analytical model to define a certain parameter using only a graph and a small number of experiments, thus taking dimensional analysis as an essential tool.

The dimensionless terms of drag and lift coefficient are defined as follows:

Drag coefficient:

$$C_D = \frac{F_D}{\frac{1}{2}\rho V^2 A} = \frac{Drag\ force}{Dynamic\ force} \quad [4]$$

Lift coefficient:

$$C_L = \frac{F_L}{\frac{1}{2}\rho V^2 A} = \frac{Lift\ force}{Dynamic\ force} \quad [5]$$

The values of the drag and lift coefficients can be observed through graphs that present the relationships of the respective coefficients for a given airfoil as a function of the angle of attack (α) and the Reynolds number (Re), which is a dimensionless number that relates the forces of inertia due to viscous forces. For better propeller performance, what is sought is to select an angle of attack where the lift coefficient is high and the drag coefficient is as low as possible.

In the case of a constant string helix, the value of the Reynolds number will undergo alterations along the extension of its radius, because the velocity V_w varies with the radius. It causes the propeller to operate outside of its project value, decreasing its efficiency.

$$Re = \frac{\rho . c . V_w}{\mu} \quad [6]$$

To maintain project conditions across the entire length of the propeller, it is necessary to design an aerodynamic profile with variable chord in order to keep the Reynolds number constant. Through an iterative method, the length of the string is calculated at a distance r from the rotor shaft.

$$c = \frac{8.\pi.r}{B.C_L}(1 - cos\varphi) \qquad [7]$$

3.1.3 Relative velocities of blade elements

Although the fluid velocity is considered constant along the length of the helix, the tangential velocity is modified as the elements differentiated by dr are analyzed. Therefore, the relative velocity of each element must be analyzed. For axial and tangential velocities, the interference factors, here called a and b, are considered. These factors are speed coefficients that are induced by the rotor.

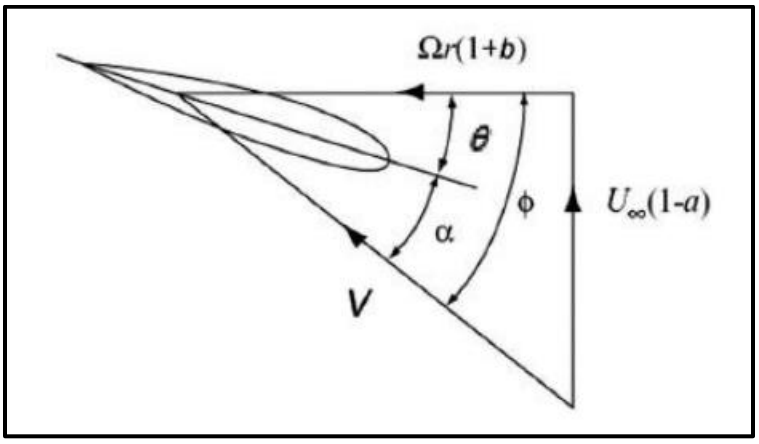

Figure 26. Relative velocities in the blade element.

By Figure 26, we obtain the important trigonometric relationships for the calculations that will be developed below.

Relative speed:

$$V = \sqrt{U^2(1-a)^2 + \Omega^2 r^2(1+b)^2} \qquad [8]$$

Flow angle:

$$\varphi = \alpha + \beta \quad [9]$$

$$tan\varphi = \frac{(1-a)}{(1+b)} . \frac{U}{\Omega . \mathrm{r}} \quad [10]$$

3.1.4 Relationship between tip speed ratio and solidity

The tip speed ratio is a dimensionless number used in calculations for propeller sizing, which denotes the relationship between the free current velocity and the tangential blade tip velocity.

$$\lambda = \frac{U}{\Omega . \mathrm{r}} \quad [11]$$

To calculate the peak speed in each element, located at a distance r, the following relationship is used, called the local peak speed ratio.

$$\lambda_r = \lambda . \frac{r}{R} \quad [12]$$

In this way, equation[10] can be written as follows:

$$tan\varphi = \frac{(1-a)}{(1+b)} . \frac{1}{\lambda_r} \quad [13]$$

In addition to this, looking at Table 3 we can find suggestions for the tip speed ratio as a function of the number of blades. These values are related to experimental results that show that propellers with fewer blades must have a higher rotational speed number to present better yields. For propellers with a high number of blades, power is more related to torque and therefore the tip speed ratio is lower.

Table 3. Ratio of tip speed to number of blades.

Tip speed ratio (λ)	Number of Blades (B)
1	08 - 24
2	06 - 12
3	03 - 06
4	03 - 04
> 4	01 - 03

Another important relationship used is solidity, which relates the area of the turbine blades to the area covered by them. For each element, local solidity is defined as:

$$\sigma = \frac{B.c}{2.\pi.r} \quad [14]$$

3.1.5 Normal and tangential forces

As already mentioned above, in the theory of shovel elements, the relations for the forces unwrapped in each element are obtained as a function of drag and lift coefficients. For a propeller with a number B of blades, each element must be considered to undergo tangential and axial stresses at a distance r from the center of the rotor. These forces can be expressed as:

$$dF_N = \frac{1}{2}.B.c.\rho.V^2.(C_L cos\varphi + C_D sin\varphi).dr \quad [15]$$

$$dF_T = \frac{1}{2}.B.c.\rho.V^2.(C_L sin\varphi - C_D cos\varphi).dr \quad [16]$$

These equations can be written in a local reference, as a function of the normal and tangential coefficient of force, according to the following relationship shown in Figure 27.

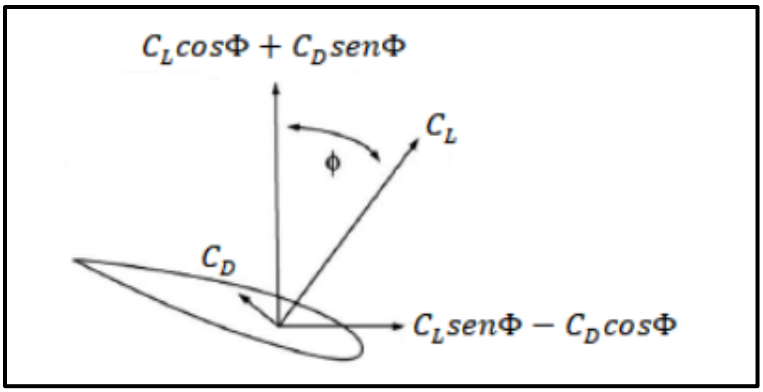

Figure 27. Decomposition of force coefficients.

Defining the normal and tangential coefficients of force as:

$$C_N = C_L cos\varphi + C_D sin\varphi \quad [17]$$

$$C_T = C_L sen\varphi - C_D cos\varphi \quad [18]$$

Equations [15] and [16] as follows:

$$dF_N = \frac{1}{2}.B.c.\rho.V^2.C_N.dr \quad [19]$$

$$dF_T = \frac{1}{2}.B.c.\rho.V^2.C_T.dr \quad [20]$$

3.2 MOMENTUM THEORY

This theory assumes that the fluid passing through the rotor eventually converts some of its energy into rotational kinetic energy. This loss results in less energy extraction by the rotor.

The unwrapped forces, considering these losses, can be calculated by this method, since the force is related to the variation of the momentum. In this theory, the rotor is divided into angular segments to proceed with the tangential and axial stress calculations of each element.

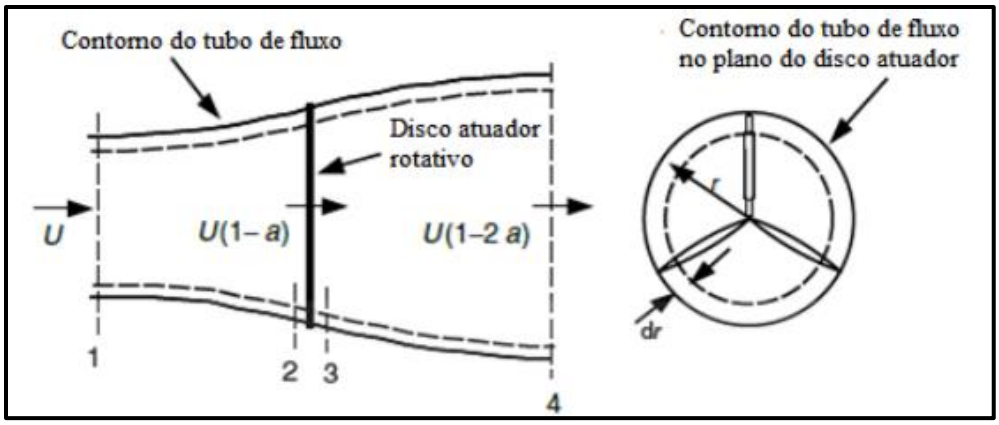

Figure 28. Geometry for rotor analysis.

For axial strength, we have:

$$dF_N = \Delta U_{axial}.d\dot{m} \quad [21]$$

$$dF_N = [U - U.(1 - 2.a)].d\dot{m} \quad [22]$$

$$dF_N = 2.U.a.d\dot{m} \quad [23]$$

Where the mass flow is given:

$$d\dot{m} = \rho.U_{axial}.(2.\pi.r.dr) \quad [24]$$

$$d\dot{m} = \rho.U.(1 - a)(2.\pi.r.dr) \quad [25]$$

Therefore, the axial force is defined by:

$$dF_N = 4.U^2.\rho.a.(1 - a).\pi.r.dr \quad [26]$$

For the tangential component of force, we have:

$$dF_T = \omega r.d\dot{m} \quad [27]$$

$$\omega = 2.\Omega.b \quad [28]$$

$$dF_T = 4.\Omega.U.\rho.(1-a).b^2.\pi.r^2.dr \quad [29]$$

3.3 THE BLADE ELEMENT MOMENTUM THEORY

The blade element momentum theory is a relation between the theory of the blades element an the momentum theory. Only by merging both it is possible to calculate the interference coefficients a and b that are induced by the rotor. The axial and tangential interference factors are not predetermined coefficients, as they depend on the characteristics of the fluid, the working regime, in addition to the chosen airfoil. Therefore, these are calculated by applying an iterative method.

Equalizing equations (19) and (26), as well as equations (20) and (29), and using some relations from Figure 26, we obtain the following relationships:

$$a = \frac{\sigma.C_N}{4.sin^2\varphi + \sigma.C_N} \quad [30]$$

$$b = \frac{\sigma.C_T}{4.sin\varphi.cos\varphi - \sigma.C_T} \quad [31]$$

The simplifications addressed in the previous theories allow the development of the blade element momentum theory, but they make this theory present some limitations. Assuming that the forces acting on the blade are exclusively in two dimensions, the orthogonal component along the blade is ignored. In addition to this, this theory does not consider the influence of losses caused by vortices at the rotor tip and cube. There are still corrections for the inclusion of these losses in the blade element theory, which are as follows.

3.4 EFFECTS OF LOSSES BY THE TIPS AND HUB OF THE ROTOR

Due to the pressure difference between the upper and lower top and bottom surfaces, the fluid tends to drain around the tip of the blade to the point of lowest pressure for the highest pressure, thus reducing the lift the production of power near the tip of the blade. This effect is referred to as lost by the tips and must be considered for more accurate results.

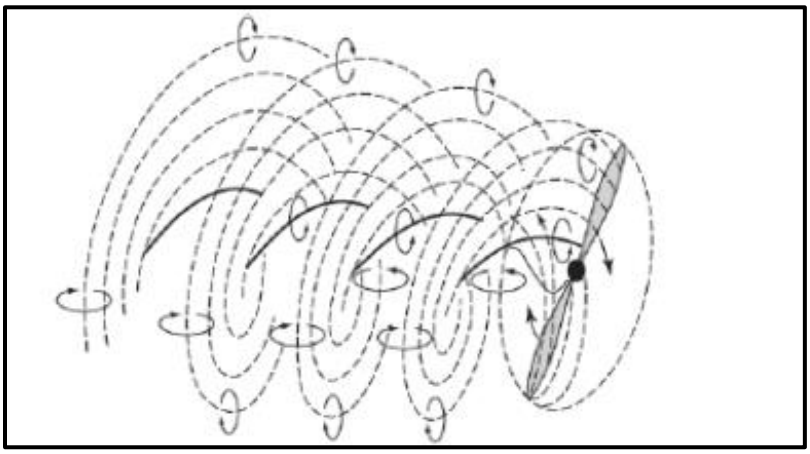

Figure 29. Effect of the losses by the tips.

Currently there are different exact solutions for the behavior of losses at the tip, such as the one proposed by Goldstein and Biot-Savart that are not widely implemented in the blade element momentum theory The Prandlt correction approximation can be used elatively easily.

$$F_{ponta} = \frac{2}{\pi}.acos\left[exp\left(-\frac{\frac{B}{2}.\left(1-\frac{r}{R}\right)}{\frac{r}{R}.sin\varphi}\right)\right] \quad [32]$$

To correct the velocity coefficients induced by the vortices present near the cube, a correction model was used in the rotor hub.

$$F_{cubo} = \frac{2}{\pi}.acos\left[exp\left(-\frac{B.(r-Ri)}{2.\pi.r.sin\varphi}\right)\right] \quad [33]$$

The product of equations (32) and (33) generate a single factor F. This factor allows considering both losses. By introducing this factor into equations (26) and (29) we obtain the new interference coefficients.

$$a = \left(1 + \frac{4.F.sin^2\varphi}{\sigma.C_L.cos\varphi}\right)^{-1} \quad [34]$$

$$b = \left(\frac{4.F.cos\varphi}{\sigma.C_L} - 1\right)^{-1} \quad [35]$$

3.5 TORQUE AND POWER

Energy conversion in the turbine occurs when the fluid kinetic energy is transformed into mechanical energy through the rotation of the rotor shaft, which occurs due to a tangential force. This force can be calculated for each element of the blade and multiplied by the distance from the element to the center of the rotor, thus obtaining what it's called torque. The product of each tangential force contribution by its respective distance gives the total torque.

$$dT = r.dF_T \quad [36]$$

The power extracted by the turbine can be described as the product of the angular speed of the rotor by the torque.

$$dP = \Omega.\mathrm{dT} \quad [37]$$

3.6 POWER COEFFICIENT

The power coefficient is a dimensionless parameter that expresses the power that can be extracted from the fluid by the turbines, this being the relationship:

$$C_P = \frac{P}{P_S} \quad [38]$$

The power available from the fluid can be calculated considering the cross-section of the turbine and the kinetic energy of the fluid.

$$P_S = \frac{1}{2}.\rho.A.U^3 \quad [39]$$

Just like wind turbines, hydraulic turbines also have limits on the amount of energy that can be extracted from the fluid. Albert Betz was the first to show that the maximum theoretical power coefficient achieved by a wind turbine is 59.3%.

$$C_{PBetz} = \frac{16}{27} = 59.3\% \quad [40]$$

This value is known as the Betz coefficient and is valid for theoretical projects that consider the following:

- Air is a homogeneous and incompressible fluid and flows in a permanent regime.
- There is no drag.
- The rotor has an infinite number of blades.
- The impulse is uniform over the entire disc area.
- There is no rotation in the wake.
- The static pressure at the inlet of the control volume is equal to the static pressure at the outlet.

3.6.1 Wake effect by rotation

The Betz coefficient is a theoretical maximum limit value of the power coefficient, regardless of the tip ratio value. Meanwhile, equation (40) is valid for high tip speed ratio values, making a significant difference for lower ratios.

For equations (36) and (37) it is observed that the torque is produced by forces tangential to the blades multiplied by their respective distances from the center of the rotor. These forces result from modifying the velocity of the fluid in a tangential direction. The direction of these fluid

airspeed modifications is opposite to the direction of the forces acting on the blades and considers that the fluid reaches the rotor without any tangential components. As a result, when passing through the rotor, the modifications of the velocities of the water occur forming a wake that rotates in the opposite direction to the rotation of the rotor, resulting in a loss of energy, since this wake still has kinetic energy of rotation.

Once the rotation decreases, a greater torque is necessary. The effect of the rotation of the wake also increases because the higher the torque, the greater the tangential speed in the wake, and consequently the lower the use of energy and power.

The following expression can be used to calculate the power coefficient including the effect of the wake rotation.

$$C_{Pideal} = \frac{16}{27}.exp(-0.35\lambda^{-1.29}) \quad [41]$$

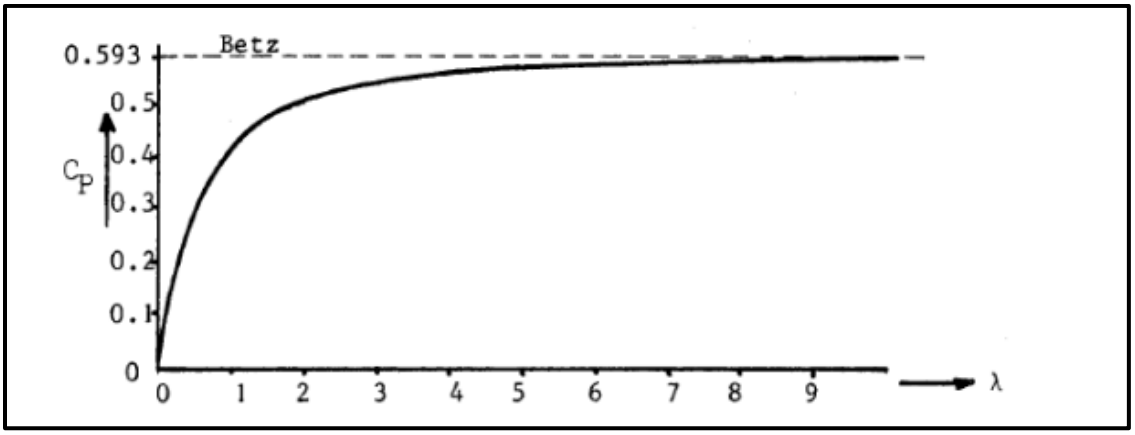

Figure 30. Power coefficient in relation to tip speed ratio.

3.6.2 Effect of the relation between drag and lift coefficient C_D/C_L ratio

The drag coefficient (C_D) is the measure of the blade's resistance to the fluid. Therefore, the relation C_D/C_L determines the losses due to this resistance. The higher the ratio, the more losses the rotor will have due to drag, resulting in loss of drag. The expression that generates the values of drag power coefficients as a function of the ratio C_D/C_L is:

$$C_{Parrastre} = \frac{16}{27} \cdot \frac{C_D}{C_L} \cdot \lambda \qquad [42]$$

Alternatively, the value can be obtained graphically:

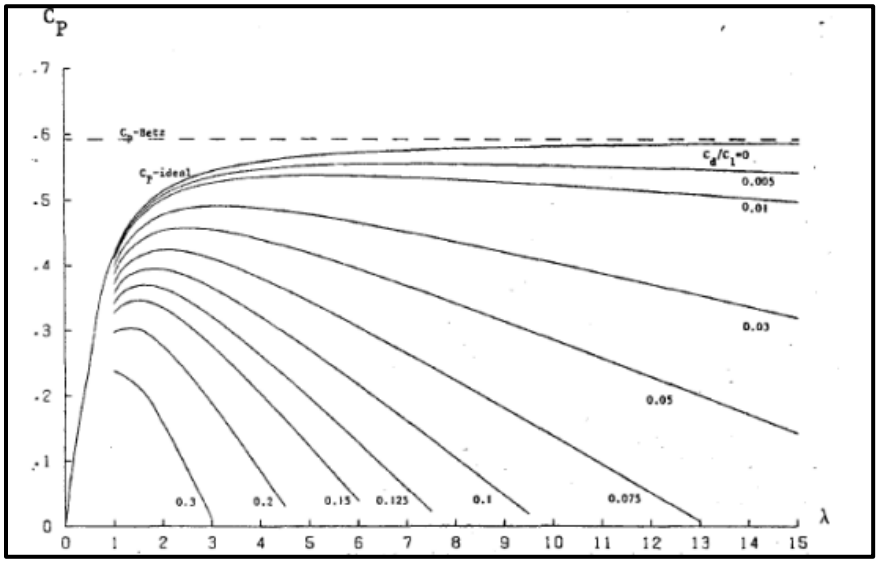

Figure 31. C_P in relation to λ with different relations Cd/Cl

3.6.3 Effect of the number of blades

In Figure 32 the curves for the power coefficient in different numbers of blades and with the relationship $^{C_D}/_{C_L} = 0{,}03$.

To draw these curves, there is an expression that defines the power reduction factor as a function of the number of blades and, consequently, in those lost by the tips.

$$\eta_B = \left(1 - \frac{1{,}386}{B} \sin\left(\frac{\varphi}{2}\right)\right)^2 \qquad [43]$$

Where in this case, φ is the value of the theoretical flow angle defined as:

$$\varphi = \frac{2}{3} arctan\left(\frac{1}{\lambda}\right) \qquad [44]$$

This flow angle is obtained when the rotation behind the rotor is not considered, and with a=0.33 and b=0.

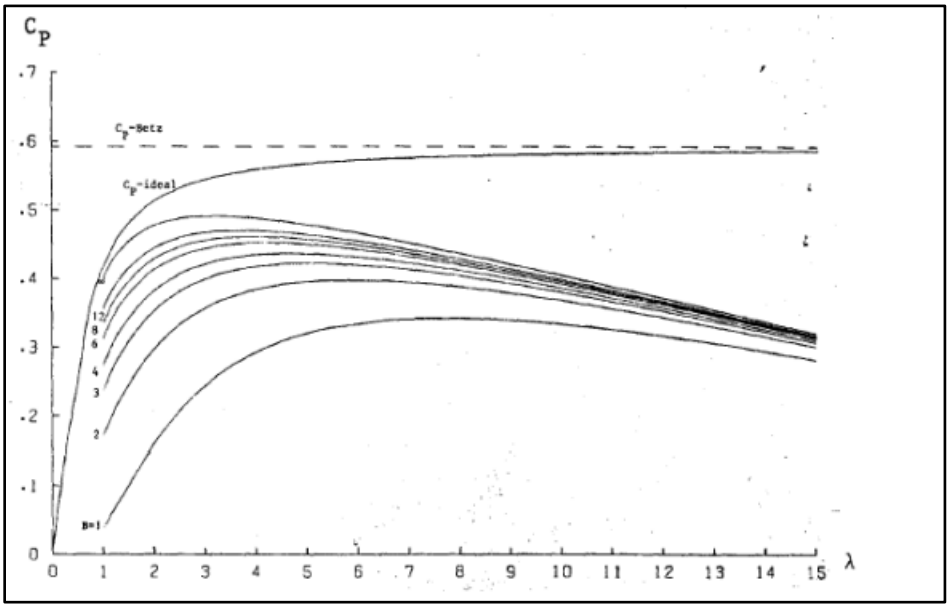

Figure 32. Effect of the number of blades on C_P according to relation λ.

3.6.4 Including all effects

Considering all the losses mentioned, it is possible to estimate the power coefficient closest to its real value.

$$C_P = \eta_B . (C_{Pideal} - C_{Parrastre}) \quad [45]$$

Replacing the terms from equation (45) with the respective expressions of the effects developed and shown in equations (41), (42) and (43), the following equation is obtained.

$$C_P = \frac{16}{27} . \left(1 - \frac{1{,}386}{B} sin\left(\frac{\varphi}{2}\right)\right)^2 \left(exp(-0{,}35\lambda^{-1{,}29}) - \frac{C_D}{C_L} . \lambda\right) \quad [46]$$

Finally, with this expression the graphs can be constructed by varying the number of blades and aerodynamic profile.

3.7 ITERATIVE METHOD

The application of the iterative method is one of the ways to calculate the parameters of a turbine, as can be seen in the literature [11] and [12]. By adopting a certain profile, angle of attack and fluid velocity it is possible to start the calculations according to the following steps.

1. Assume initial values of a and b.
2. Divide the propeller into n sections.
3. Determine the flow angle and the angle of attack.
4. Determine the chord.
5. Determine the axial and tangential coefficients.
6. Calculate the local solidity.
7. Determine the values a and b, returning to step 1 and doing the iterative step until convergence.
8. Determine the velocity U and angular velocity.
9. Determine the axial and tangential forces.
10. Determine torque and power.
11. Repeat the procedure for all the elements of the blade and then, by summing all the contributions of each element, find the torque and the total power.

Parameters a and b are independent variables. There are limiting constraints on interference coefficient values for the application of the momentum theory of the blade element. The maximum value of the axial coefficient a is 0.5. A higher value would imply that the flow would be reversed.

In Souza's literature [1], he makes use of his own code following these steps in order to determine the parameters of an optimized 10-blade propeller. In this work we will make use of this design to be able to obtain a conclusion of what happened by reducing the number of blades from 10 to 3 without modifying the chord values **(objective 6).**

4. DEVELOPMENT OF THE PROJECT

4.1 PROJECT PARAMETERS

The project parameters will vary in accordance with the objectives set out in this work. In order to carry out a comparative analysis with the Souza project [1] we will use the same fundamental parameters:

Table 4. Fundamental parameters of the project.

Description	Symbol	Value
Profile	-	NACA 6409
Angle of attack	α	11°
Lift coefficient	C_L	1,3
Drag coefficient	C_D	0,05
Fluid velocity	U	0.7 m/s
Specific mass of water	ρ	999 kg/m^3
Rotor diameter	D_e	0.05 m
Cube diameter	D_i	0.01 m

For **objective 1** we will use our own code which was based on the algorithm developed by Junior [11] and validated by Souza [1]. For the verification of this code, the parameters used in Souza were used to [1] in the non-optimized propeller.

Table 5. Souza parameters.

Description	Symbol	Value
Profile	-	NACA 6409
Angle of attack	α	11°
Lift coefficient	C_L	1,3
Drag coefficient	C_D	0,05
Fluid velocity	U	0.7 m/s
Specific mass of water	ρ	999 kg/m^3

Rotor diameter	D_e	0.05 m
Cube diameter	D_i	0.01 m
Number of blades	B	10
Tip speed ratio	λ	1

This code will not take into account the factors of interference, that is, we will start the code assuming a=0 and b=0.

The choice of the airfoil is based on the criterion of achieving comparability with Souza's project [1], which in turn is compared with Fernández's work [13].

The chosen profile is a NACA 6409 which provides a good lift coefficient and low drag coefficient at a given angle of attack.

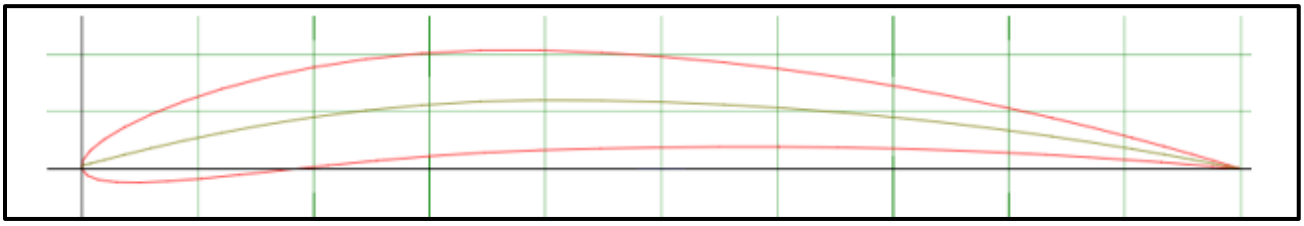

Figure 33. NACA 6409 profile geometry.

Making use of the graphics provided by NACA, we will look for the angle of attack that provides us with the lowest drag coefficient and the highest lift coefficient, that is, we will achieve the highest upward thrust force (Lift force) getting the lowest drag force (Drag force). We can see this in the following Figures, both in Figure 34 and in Figure 35.

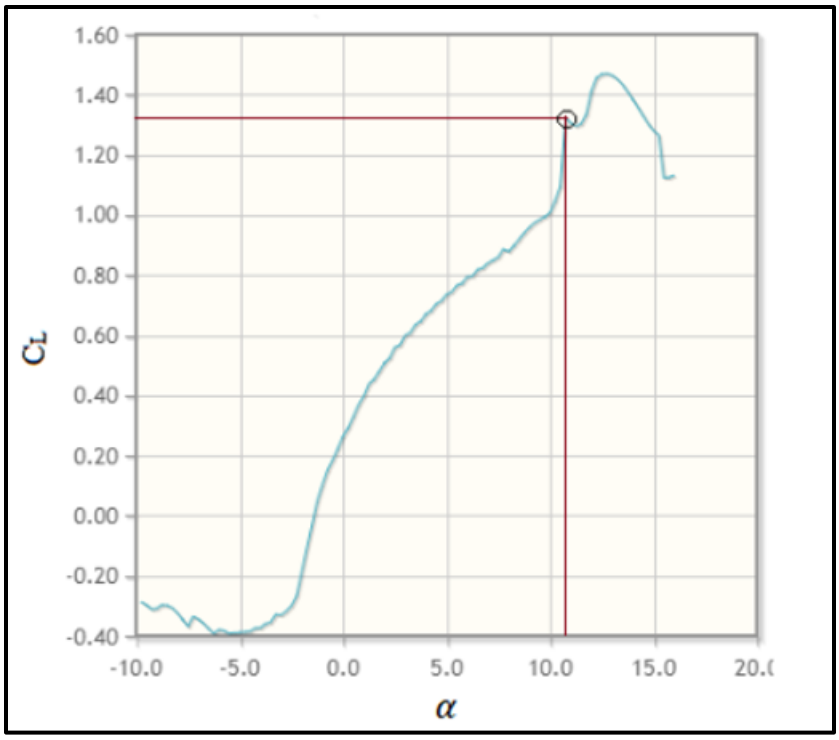

Figure 34. Curve of C_L in relation to the angle of attack NACA 6409.

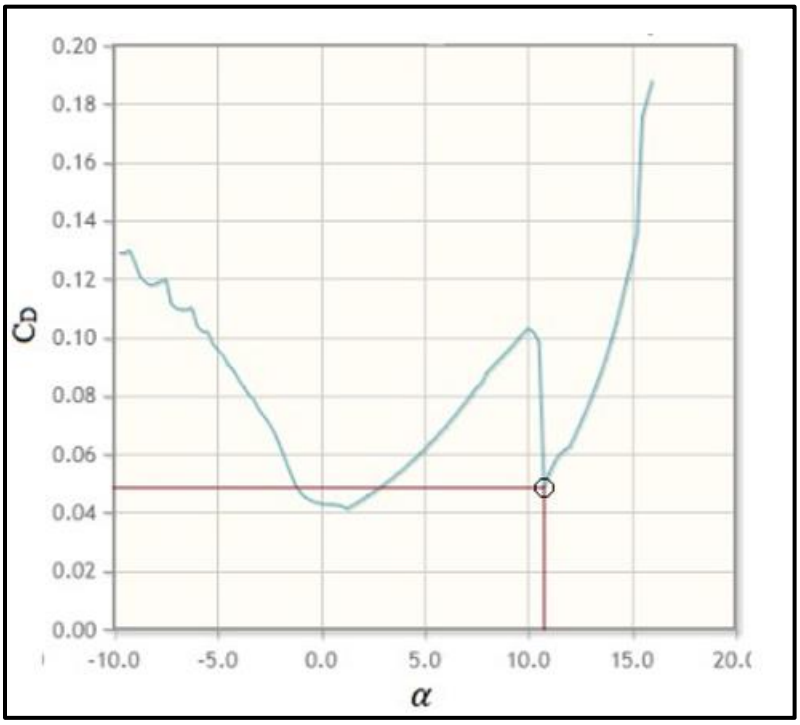

Figure 35. C_D curve in relation to the angle of attack NACA 6409.

The diameter of the selected rotor is the same as that of Souza [1], this is not only to achieve an accurate comparison but also for the ease of printing and testing at scale without the use of 3D printing machines and water channel of greater dimensions, thus, making use of the machinery available in ESTIG and its laboratories.

For the internal diameter, that is, that of the cube, it must be between 15% and 20% according to Fernández [13]. The theoretical specific mass of water, a value was chosen based on a water temperature around 15°C, this value varies non-linearly depending on the temperature; 15°C is a standard use value.

Taking into account **objective 2,** we will do different tests with different values of tip speed ratio to be able to endorse a comparison between them and conclude in the influence of this parameter. According to Table 3 values in which values of λ are recommended as a function of variable B were obtained.

The results for the power available by the fluid and power coefficient were obtained through equations (39) and (46) respectively. The power of the turbine is given by equations (38). Finally, the torque is calculated through equation (37) by dividing it by the rotation in rad/s.

The code of **objective 1** was developed using the Excel program, making use of the parameters proposed above. To start the code, we only need to make use of the following values:

- Angle of attack.
- Lift coefficient.
- Rotor diameter.
- Diameter of the cube.
- Number of blades.
- Tip speed ratio.

In this code, the axial (a) and tangential (b) interference values are considered null. The blade was divided into 15 elements to achieve a well-defined profile and avoid further smoothing.

Table 6. Input data.

Input data			
Name	Symbol	Value	
Profile	-	6409	-
Anfle of attack	α	11	°
Lift coefficient	CL	1,3	-
Drag coefficient	CD	0,06	-
Fluid velocity	U	0,78	m/s
Specific mass of water	ρ	999	kg/m3
Rotor diameter	De	50	mm
Cube diameter	Di	10	mm
Number of blades	B	3	-
Cross section	A	0,0019635	m2
Tip speed ratio	λ	1	-

Once the parameters have been entered, the first calculation to be made is the division of the blade elements taking into account the number of divisions, rotor diameter (D_e) and cube diameter (D_i).

Then, we proceed to the calculation of the local tip speed ratio (λ_r), making use of the chosen tip speed ratio (λ).

With these values already calculated, we proceed to the calculation of the flow angle (φ) and then together with the value of the angle of attack (α) obtain the value of the pitch angles (β). Finally, we obtain the value of the chord (c) for that element, by using the values of number of blades (B), coefficient of lift (C_L), flow angle (φ) and radius corresponding to the element (r).

Table 7. Example of result.

a=0 b=0						
Element	radius r (m)	Local tip speed ratio λr	Flow angle ϕ (°)	Pitch angle β (°)	Chord (m)	Chord (mm)
1	0,005000	0,2	78,69	67,69	0,025902	25,9023
2	0,0064	0,3	75,58	64,58	0,031110	31,1104
3	0,0079	0,3	72,55	61,55	0,035452	35,4524
4	0,0093	0,4	69,62	58,62	0,039004	39,0044
5	0,0107	0,4	66,80	55,80	0,041847	41,8474
6	0,0121	0,5	64,09	53,09	0,044063	44,0635
7	0,0136	0,5	61,50	50,50	0,045733	45,7326
8	0,0150	0,6	59,04	48,04	0,046931	46,9310
9	0,0164	0,7	56,69	45,69	0,047729	47,7288
10	0,0179	0,7	54,46	43,46	0,048190	48,1897
11	0,0193	0,8	52,35	41,35	0,048370	48,3704
12	0,0207	0,8	50,36	39,36	0,048321	48,3206
13	0,0221	0,9	48,47	37,47	0,048083	48,0832
14	0,0236	0,9	46,68	35,68	0,047695	47,6950
15	0,025000	1,0	45,00	34,00	0,047187	47,1872

For **objective 2,** using the code described above, different tip speed ratio (λ) values will be used in a range of [1; 5]. In practice, because for values of λ greater than 3 the lengths of the string become small in scale to the possibility of carrying out a 3D printing correctly, λ values will be used in a range [1;3].

Table 3 indicates that for 3 blade propellers the recommended value of λ is 5. Having said the above, it is difficult to print a propeller with this parameter.

Objective 3 consists of obtaining the CAD of the propellers that will then be sent to the FabLab laboratory for printing (**objective 4**). These designs as already mentioned were carried out through the SolidWorks assisted design program.

To obtain these designs, the aerodynamic profile of the NACA page is imported, once the profile has been obtained in a sketch, the dimension of the chord and angle of attack are limited. As we already know the angle of attack is fixed but the string varies from section to section, values that we obtain from the code and we must insert in each sketch for each section. Already in the final phase, an extrusion is made with the coating tool and our initial blade is formed.

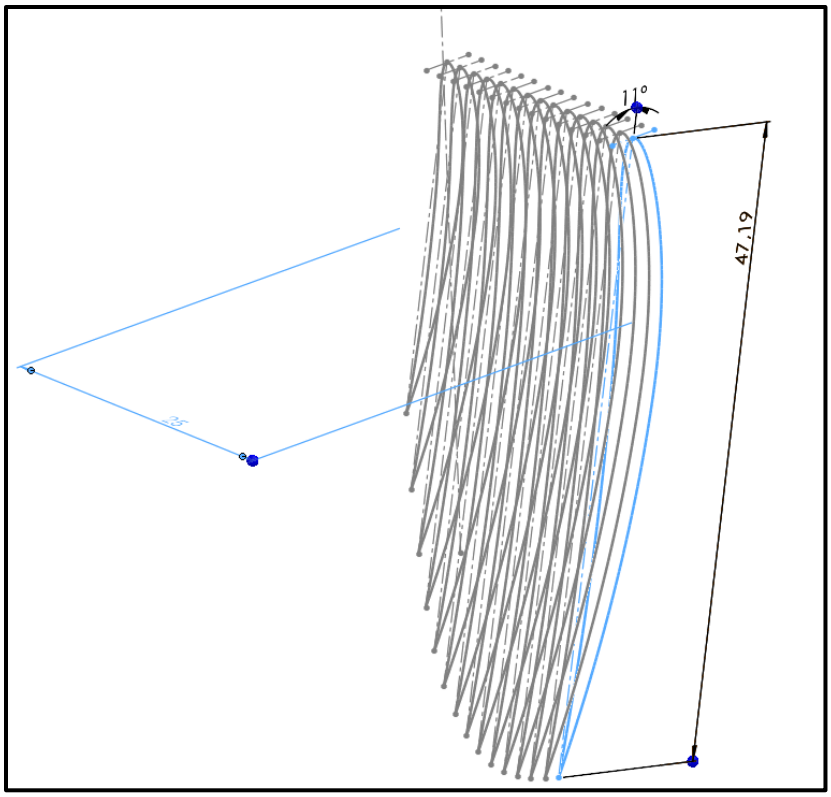

Figure 36. Sketch of a blade.

Finally, a circular matrix is generated with the number of blades needed.

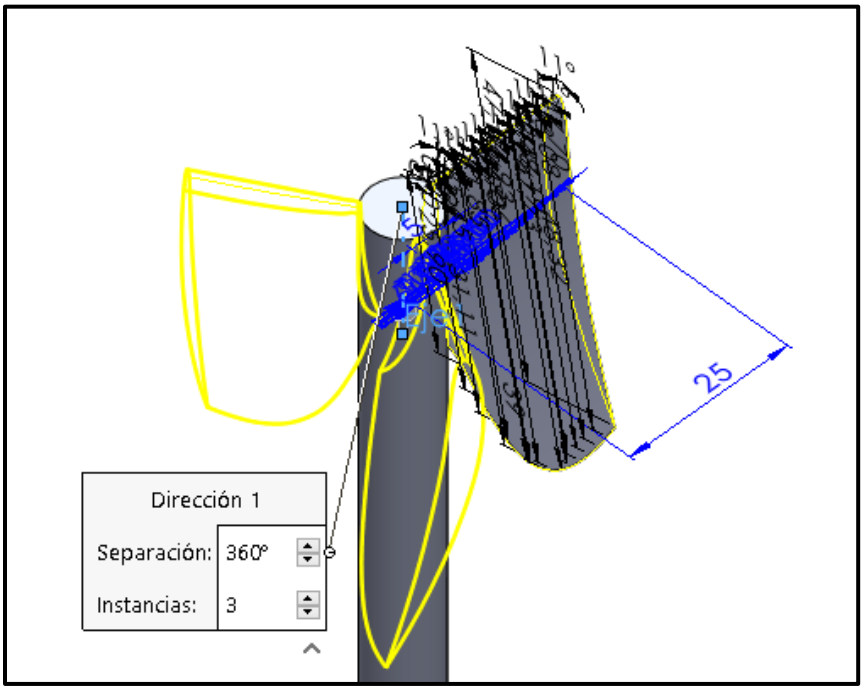

Figure 37. Circular matrix.

4.2 GENERATION OF BLADE ELEMENTS

4.2.1 Propeller 1 with a=0 and b=0 of 3 blades

For the generation of the propeller without interference factor of 3 blades, we will start from the model developed by Souza [1] which has a value of the parameter B=10.

With this data we will basically reduce the value of blades from 10 to 3 in the SolidWorks design program. This is achieved by reducing the parameter of the circular matrix. The purpose of this is to be able to reach a conclusion by varying the value B without modifying the values of the code. In this case Souza [1] makes use of 5 elements.

Table 8. Blade elements for Propeller a=0 b=0.

Element	Radius r (m)	Tip speed ratio λ	Flow angle φ (°)	Pitch angle β (°)	Chord (m)
1	0,005	0,2	78,69	67,69	0,00777
2	0,01	0,4	68,20	57,20	0,01215
3	0,015	0,6	59,04	48,04	0,01408
4	0,02	0,8	51,34	40,34	0,01451
5	0,025	1	45,00	34,00	0,01415

Once the calculation is complete, the 3D design is carried out through the SolidWorks design program.

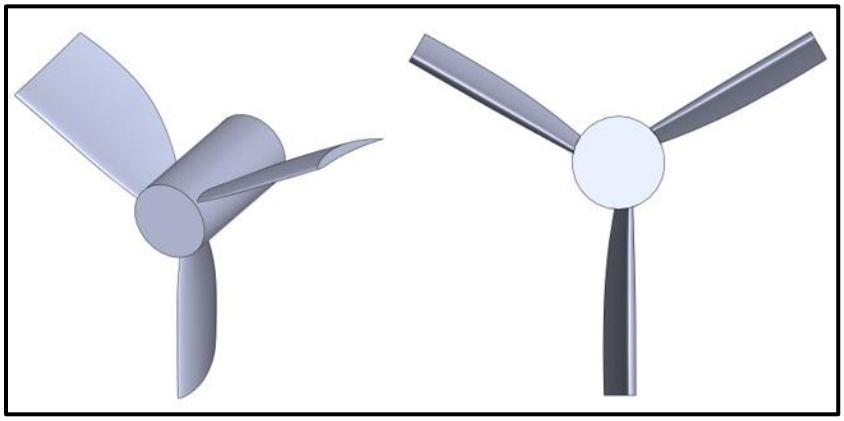

Figure 38. Propeller 1 a=0 b=0.

4.2.2 Propeller 2 with a≠0 and b≠0 of 3 blades

For the generation of the propeller with interference factor of 3 blades, we will start from the model developed by Souza [1] which has a value of the parameter B=10.

With this data we will basically reduce the value of blades from 10 to 3 in the SolidWorks design program. This is achieved by reducing the parameter of the circular matrix. The purpose of this is to be able to reach a conclusion by varying the value B without modifying the values of the code. In this case Souza [1] makes use of 5 elements.

Table 9. Blade elements for Propeller a≠0 b≠0.

Element	Radius r (m)	Tip speed ratio λ	Flow angle φ (°)	Pitch angle β (°)	Chord (m)
1	0,005	0,2	84,18	73,18	0,00868
2	0,01	0,4	78,86	67,86	0,01560
3	0,015	0,6	74,54	63,54	0,02127
4	0,02	0,8	70,19	59,19	0,02556
5	0,025	1	45,00	34,00	0,01415

Once the calculation is complete, the 3D design is carried out through the SolidWorks design program.

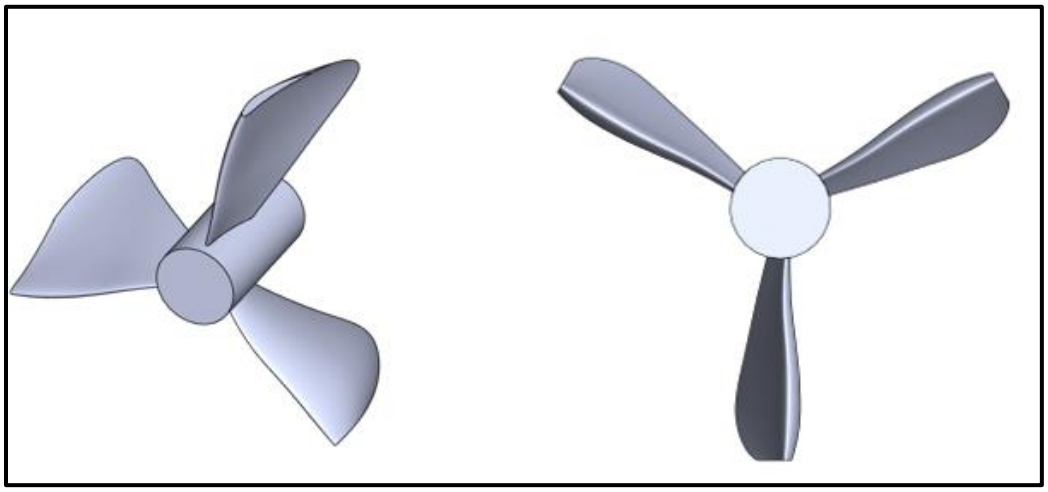

Figure 39. Propeller 2 a≠0 b≠0.

4.2.3 Propeller 3 without interference factor with 3 blades λ=1

For the calculation of the propeller without interference factor with 3 blades and tip speed ratio λ=1, a proprietary code developed in the Excel program was used as already explained above.

The input data are as follows:

Table 10. Input data B=3 λ=1.

Input data			
Name	Symbol	Value	
Profile	-	6409	-
Anfle of attack	α	11	°
Lift coefficient	CL	1,3	-
Drag coefficient	CD	0,06	-
Fluid velocity	U	0,78	m/s
Specific mass of water	ρ	999	kg/m3
Rotor diameter	De	50	mm
Cube diameter	Di	10	mm
Number of blades	B	3	-
Cross section	A	0,0019635	m2
Tip speed ratio	λ	1	-

Yielding the following results.

Table 11. Result B=3 λ=1.

a=0 b=0						
Element	radius r (m)	Local tip speed ratio λr	Flow angle ϕ (°)	Pitch angle β (°)	Chord (m)	Chord (mm)
1	0,005000	0,2	78,69	67,69	0,025902	25,9023
2	0,0064	0,3	75,58	64,58	0,031110	31,1104
3	0,0079	0,3	72,55	61,55	0,035452	35,4524
4	0,0093	0,4	69,62	58,62	0,039004	39,0044
5	0,0107	0,4	66,80	55,80	0,041847	41,8474
6	0,0121	0,5	64,09	53,09	0,044063	44,0635
7	0,0136	0,5	61,50	50,50	0,045733	45,7326
8	0,0150	0,6	59,04	48,04	0,046931	46,9310
9	0,0164	0,7	56,69	45,69	0,047729	47,7288
10	0,0179	0,7	54,46	43,46	0,048190	48,1897
11	0,0193	0,8	52,35	41,35	0,048370	48,3704
12	0,0207	0,8	50,36	39,36	0,048321	48,3206
13	0,0221	0,9	48,47	37,47	0,048083	48,0832
14	0,0236	0,9	46,68	35,68	0,047695	47,6950
15	0,025000	1,0	45,00	34,00	0,047187	47,1872

Once the calculation is complete, the 3D design is carried out through the SolidWorks design program.

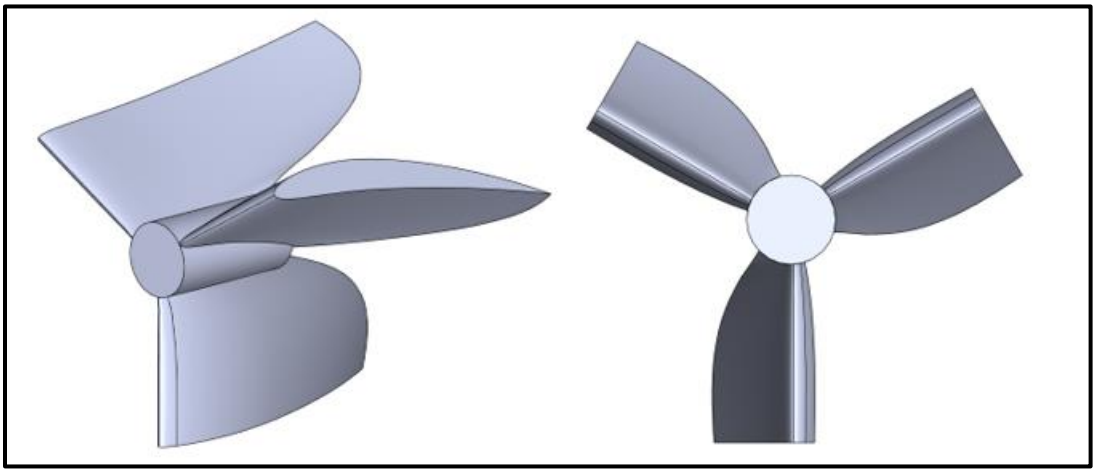

Figure 40. Propeller 3 a≠0 b≠0 λ=1.

4.2.4 Propeller 4 without interference factor with 3 blades λ=2

For the calculation of the propeller without interference factor with 3 blades and tip speed ratio λ=2, a proprietary code developed in the Excel program was used as explained above.

The input data are as follows:

Table 12. Input data B=3 λ=2.

Input data			
Name	Symbol	Value	
Profile	-	6409	-
Anfle of attack	α	11	°
Lift coefficient	CL	1,3	-
Drag coefficient	CD	0,06	-
Fluid velocity	U	0,78	m/s
Specific mass of water	ρ	999	kg/m3
Rotor diameter	De	50	mm
Cube diameter	Di	10	mm
Number of blades	B	3	-
Cross section	A	0,0019635	m2
Tip speed ratio	λ	2	-

Yielding the following results.

Table 13. Result B=3 λ=2.

a=0 b=0						
Element	radius r (m)	Local tip speed ratio λr	Flow angle ϕ (°)	Pitch angle β (°)	Chord (m)	Chord (mm)
1	0,005000	0,4	68,20	57,20	0,020255	20,2547
2	0,0064	0,5	62,78	51,78	0,022481	22,4808
3	0,0079	0,6	57,85	46,85	0,023688	23,6879
4	0,0093	0,7	53,39	42,39	0,024156	24,1559
5	0,0107	0,9	49,40	38,40	0,024111	24,1115
6	0,0121	1,0	45,83	34,83	0,023727	23,7272
7	0,0136	1,1	42,65	31,65	0,023129	23,1288
8	0,0150	1,2	39,81	28,81	0,022405	22,4047
9	0,0164	1,3	37,27	26,27	0,021616	21,6157
10	0,0179	1,4	34,99	23,99	0,020802	20,8022
11	0,0193	1,5	32,95	21,95	0,019991	19,9905
12	0,0207	1,7	31,11	20,11	0,019197	19,1974
13	0,0221	1,8	29,45	18,45	0,018433	18,4327
14	0,0236	1,9	27,94	16,94	0,017702	17,7022
15	0,025000	2,0	26,57	15,57	0,017009	17,0086

Once the calculation is complete, the 3D design is carried out through the SolidWorks design program.

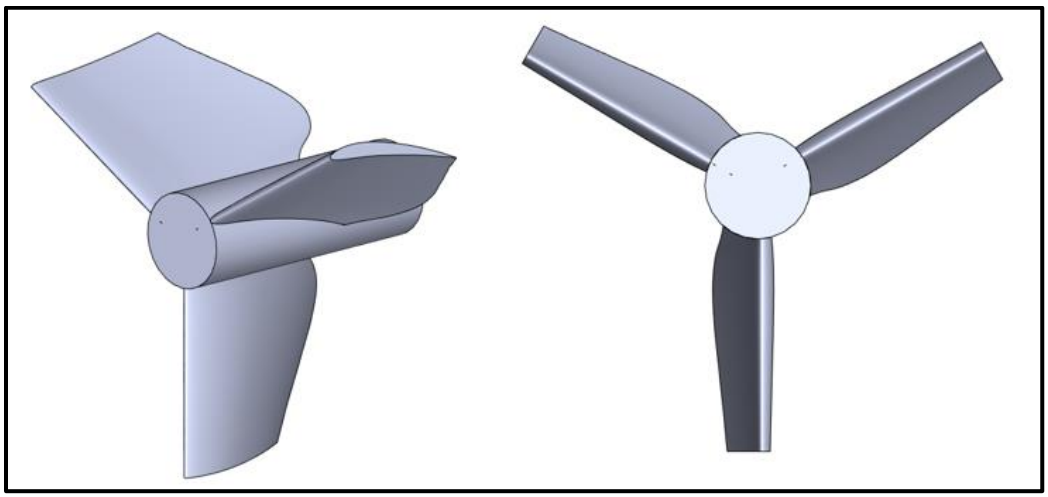

Figure 41. Propeller 4 a≠0 b≠0 λ=2.

4.2.5 Propeller 5 without interference factor with 3 blades λ=3

For the calculation of the propeller without interference factor with 3 blades and tip speed ratio λ = 3, a proprietary code developed in the Excel program was used as explained above.

The input data are as follows:

Table 14. Input data B=3 λ=3.

Input data			
Name	Symbol	Value	
Profile	-	6409	-
Anfle of attack	α	11	°
Lift coefficient	CL	1,3	-
Drag coefficient	CD	0,06	-
Fluid velocity	U	0,78	m/s
Specific mass of water	ρ	999	kg/m3
Rotor diameter	De	50	mm
Cube diameter	Di	10	mm
Number of blades	B	3	-
Cross section	A	0,0019635	m2
Tip speed ratio	λ	3	-

Yielding the following results.

Table 15. Result B=3 λ=3.

a=0 b=0						
Element	radius r (m)	Local tip speed ratio λr	Flow angle ϕ (°)	Pitch angle β (°)	Chord (m)	Chord (mm)
1	0,005000	0,6	59,04	48,04	0,015644	15,6437
2	0,0064	0,8	52,35	41,35	0,016123	16,1235
3	0,0079	0,9	46,68	35,68	0,015898	15,8983
4	0,0093	1,1	41,91	30,91	0,015305	15,3045
5	0,0107	1,3	37,87	26,87	0,014544	14,5444
6	0,0121	1,5	34,46	23,46	0,013732	13,7322
7	0,0136	1,6	31,55	20,55	0,012929	12,9288
8	0,0150	1,8	29,05	18,05	0,012165	12,1645
9	0,0164	2,0	26,90	15,90	0,011452	11,4523
10	0,0179	2,1	25,02	14,02	0,010796	10,7961
11	0,0193	2,3	23,37	12,37	0,010195	10,1951
12	0,0207	2,5	21,91	10,91	0,009646	9,6460
13	0,0221	2,7	20,62	9,62	0,009145	9,1446
14	0,0236	2,8	19,47	8,47	0,008687	8,6866
15	0,025000	3,0	18,43	7,43	0,008267	8,2675

Once the calculation is complete, the 3D design is carried out through the SolidWorks design program.

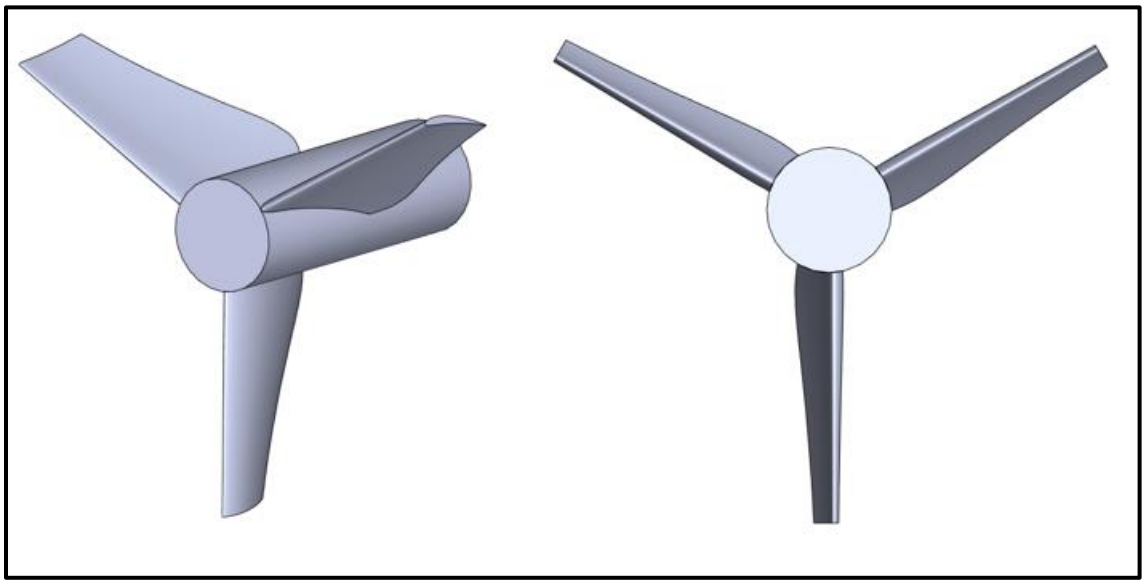

Figure 42. Propeller 5 a≠0 b≠0 λ=3.

4.3 3D PRINTING

The 3D prints of the propellers previously modeled in the SolidWorks commercial program were made by the laboratory located at the Polytechnic Institute of Braganza – ESTIG, FabLab.

In order to achieve the coupling of the propeller to the base, which we will describe later, an axis of 5mm in diameter and 150mm in length was introduced to the design, ensuring that this value is sufficient to be able to leave the propeller in a position away from any object, either to the base itself and the walls of the experimentation tunnel in order to avoid disturbances that could modify the values obtained during the practice.

The propellers were printed using Fused Deposition Modeling (FDM) technology, using the Cura slicer and using the Ultimaker model *3* extended printer.

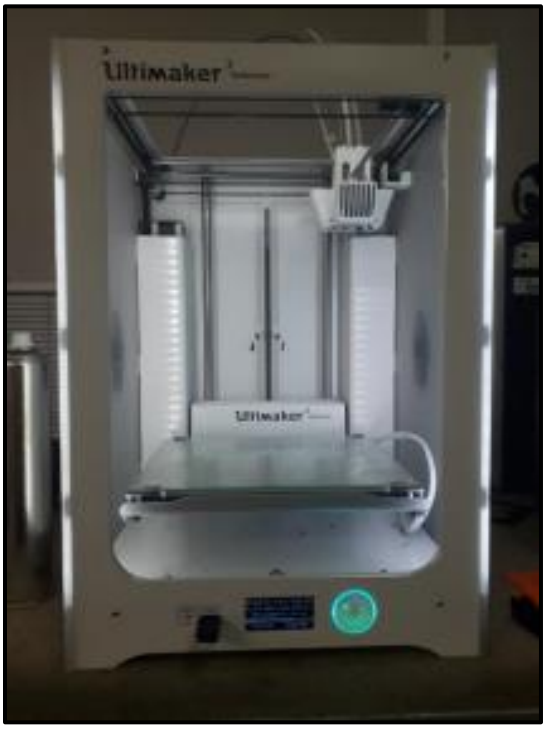

Figure 43. Ultimaker 3 Extended.

Due to the low mechanical demands that this experimentation will demand, either due to the magnitude of the scale and power developed, the prints were carried out by using the L-polylactic acid material better known in the field as PLA. This is one of the most used materials in 3D printing, not only for its versatility, but for its low cost and ease of printing.

Next, the mechanical properties of this filament will be detailed, this has been provided by the Ultimaker brand site [27].

	Test method	Typical value		
		XY (Flat)	YZ (Side)	Z (Up)
Tensile (Young's) modulus	ASTM D3039 (1 mm / min)	3250 ± 119 MPa	3292 ± 101 MPa	3071 ± 181 MPa
Tensile stress at yield	ASTM D3039 (5 mm / min)	52.5 ± 0.9 MPa	59.0 ± 0.7 MPa	No yield
Tensile stress at break	ASTM D3039 (5 mm / min)	45.5 ± 1.1 Mpa	56.0 ± 1.5 MPa	33.1 ± 2.8 MPa
Elongation at yield	ASTM D3039 (5 mm / min)	3.4 ± 0.0%	3.4 ± 0.1%	No yield
Elongation at break	ASTM D3039 (5 mm / min)	7.8 ± 1.2%	4.2 ± 0.7%	2.0 ± 0.2%
Flexural modulus	ISO 178 (1 mm / min)	3019 ± 87 MPa	2894 ± 53 MPa	2740 ± 47 MPa
Flexural strength	ISO 178 (5 mm / min)	96.8 MPa at 2.5% strain	101.3 MPa at 1.1% strain	52.0 MPa at 4.4% strain
Flexural strain at break	ISO 178 (5 mm / min)	4.8 ± 0.2%	No break (>10%)	1.9 ± 0.2%
Charpy impact strength (at 23 °C)	ISO 179-1 / 1eB (notched)	3.9 ± 0.4 kJ/m²	–	–
Hardness	ISO 7619-1 (Durometer, Shore D)	84 Shore D	–	–

Figure 44. Mechanical properties of PLA Ultimaker.

In Figure 45 the printed propellers, from left to right upwards [1 to 5].

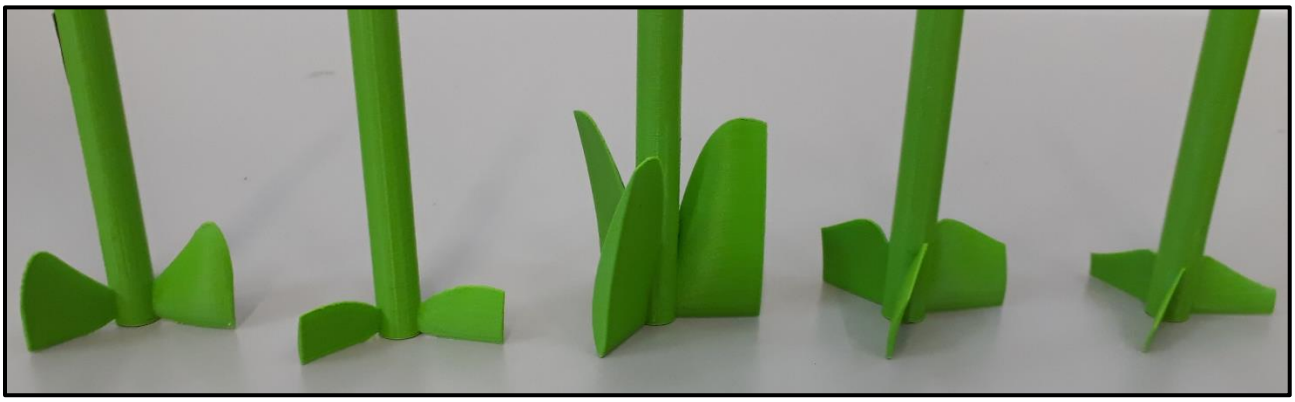

Figure 45. Propellers manufactured by 3D printing.

Below are detailed Figures of each propeller already in the fluid mechanics laboratory.

4.3.1 Propeller 1

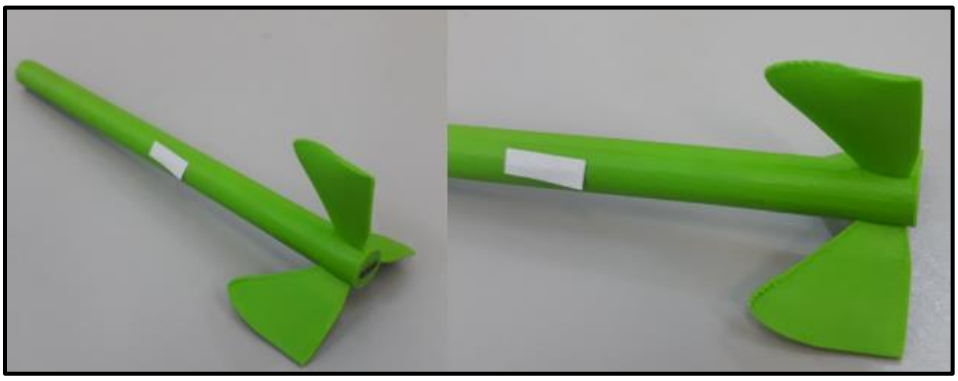

Figure 46. Propeller 1.

4.3.2 Propeller 2

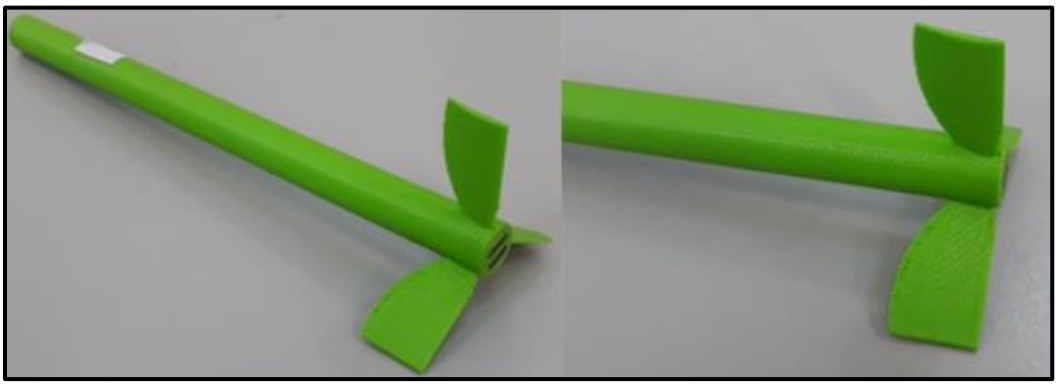

Figure 47. Propeller 2.

4.3.3 Propeller 3

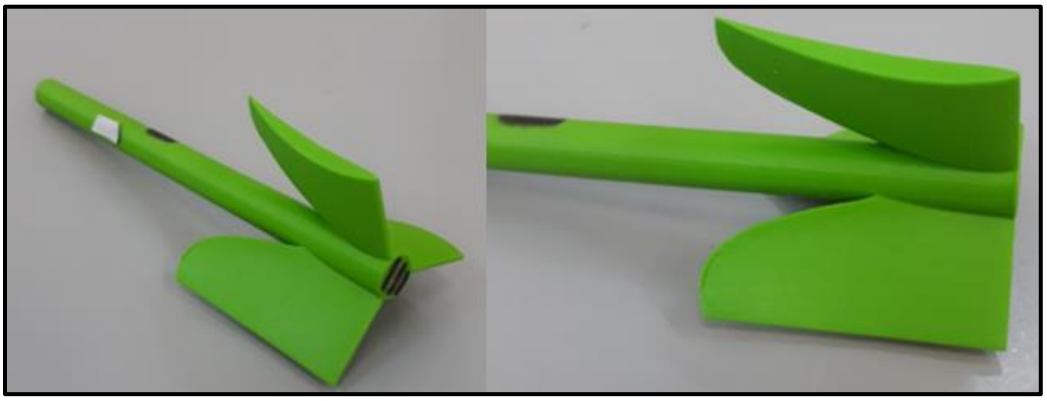

Figure 48. Propeller 3.

4.3.4 Propeller 4

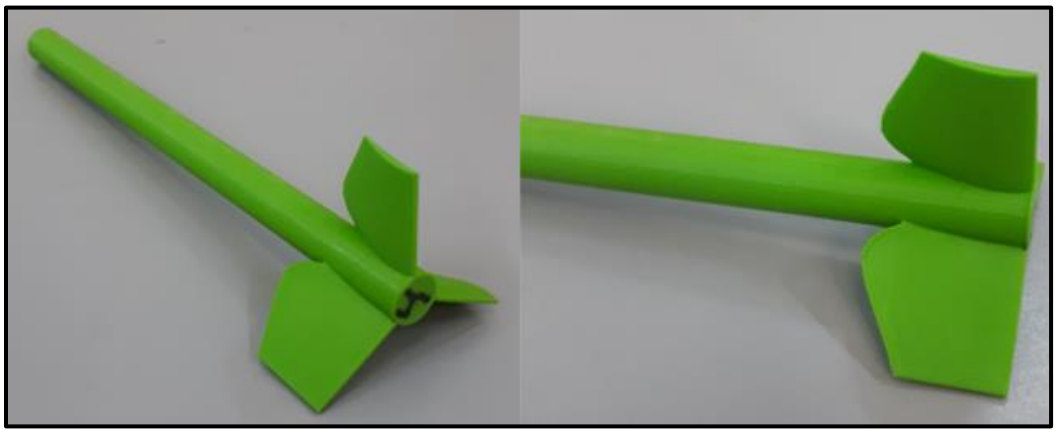

Figure 49. Propeller 4.

4.3.5 Propeller 5

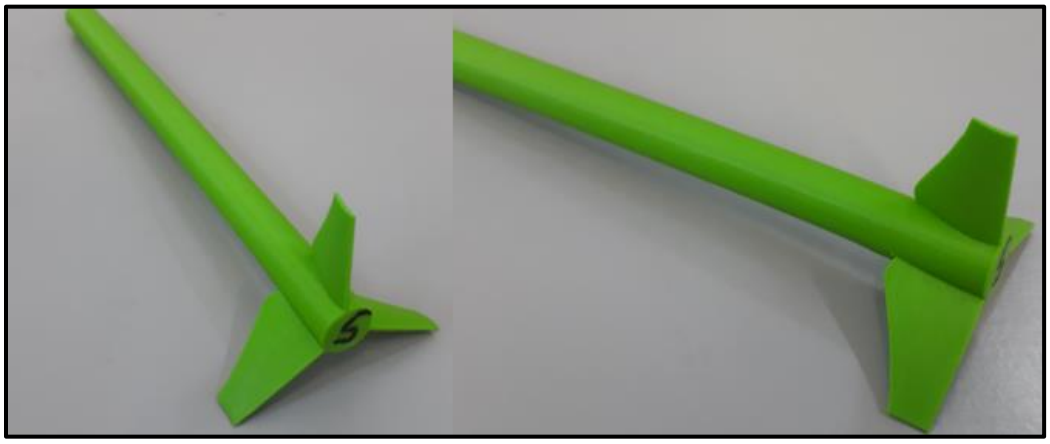

Figure 50. Propeller 5.

5. EXPERIMENTATION

Once the modeling parameters, the design, and the impressions achieved have been obtained, we will give way to experimentation. We will explain in this chapter the materials used, equipment and limitations.

All tests were conceived at the IPB-ESTIG, in the fluid mechanics laboratory.

5.1 MATERIALS AND EQUIPMENT

With the certainty that this work aims to compare results obtained from the Souza project [1], the same test elements will be used and it will be sought to do so through the same conditions of use to achieve that these are comparable.

5.1.1 Hydraulic channel

The main equipment used is the hydraulic water channel of the manufacturer Engineering Laboratory Design (ELD), which will not allow to recreate the conditions of use of the propeller by means of a constant flow obtained from a centrifuge type pump. This recreates the bed of a river.

Figure 51. Hydraulic water channel label.

Figure 52. Hydraulic channel located in the fluid mechanics laboratory.

In order to increase the depth of this artificial channel in order to achieve the complete immersion of the propeller, a fiberglass spillway section provided by the manufacturer is used.

Figure 53. Spillway section.

Technical data of the channel/pump:

- Engineering Laboratory Design inc. (ELD).
- 1 HP.
- 1425 RPM.
- Channel length 2.20 meters.
- Fiberglass spillway section.

The flow is generated by a LEESON brand pump.

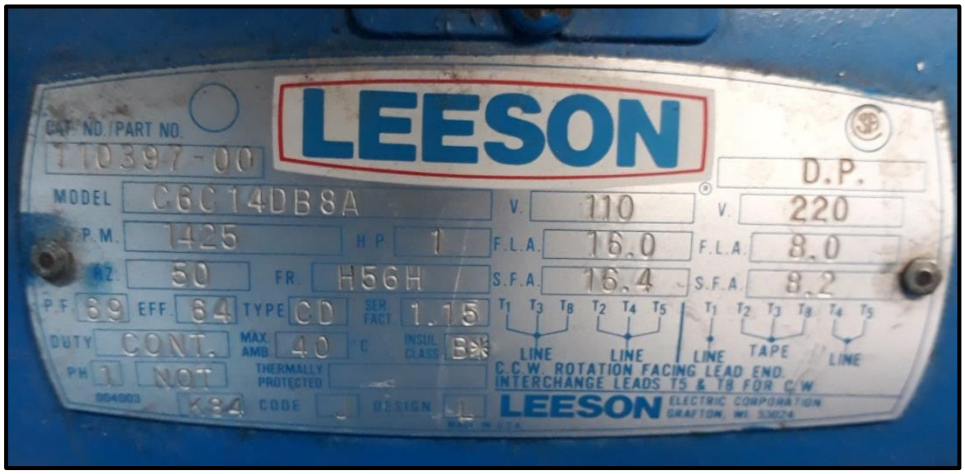

Figure 54. Characteristic sheet of the pump.

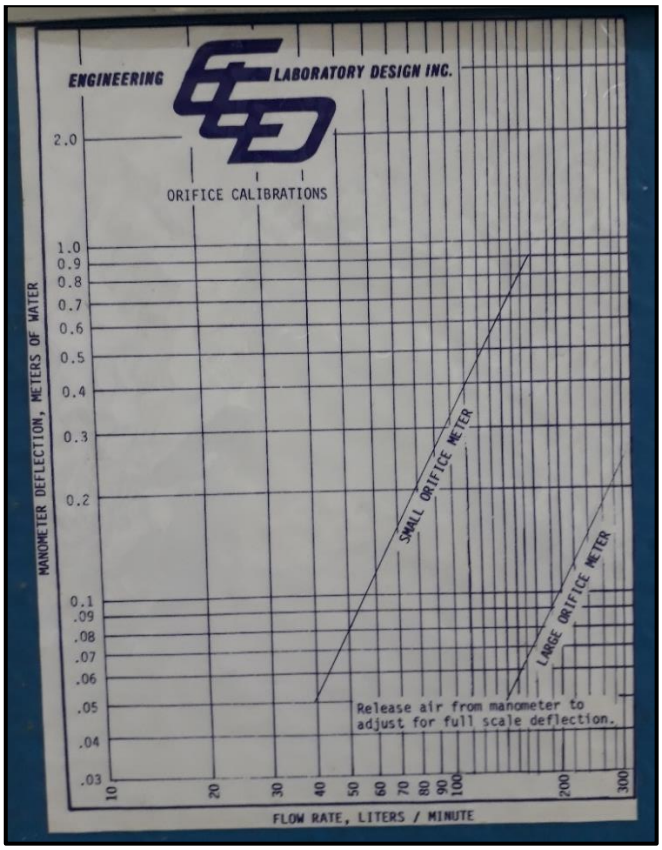

Figure 55. Manometer / flow rate chart

5.1.2 Miniturbine base

The base of the mini turbine has as its main objective to simulate the equipment where the propeller will be placed in a real case, this base has been built taking into account the necessary clearance to be able to couple the propeller / axle to an adequate height and position thus facilitating the full use of the flow generated.

The shaft will be coupled to a sealed bearing, which will keep friction losses as low as possible.

The main plate of the base has as an addition 4 screws that will act as leveling elements, if necessary, they also provide additional weight to ensure that the base next to the propeller remains stable during the test.

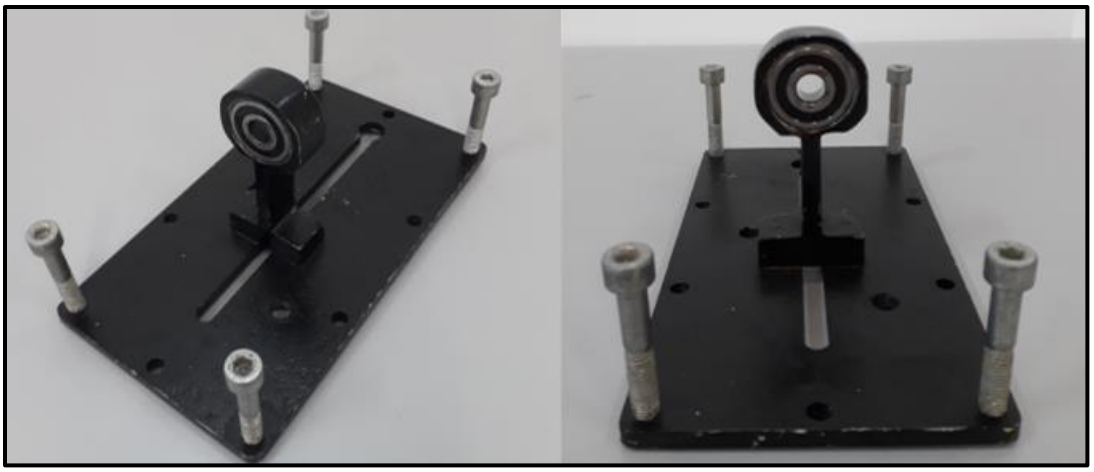

Figure 56. Mini turbine base.

5.1.3 Tachometer

The tachometer will be used to read the only parameter that we are going to obtain from the test directly (in addition to the difference in water column), the Propeller Revolutions (RPM).

This will be a digital tachometer of the RS brand, which is available in IPB laboratories.

Figure 57. RS Tachometer.

Technical data:

- RS PRO.
- [0.5 ; 100] RPM.
- 0.1 RPM Resolution.

Accessory: Contact wheel.

For the use of this, the tachometer will be used in photo mode and by means of a reflective tape provided by the same tachometer, which will be placed on the axis of the propeller, the measurements will be made.

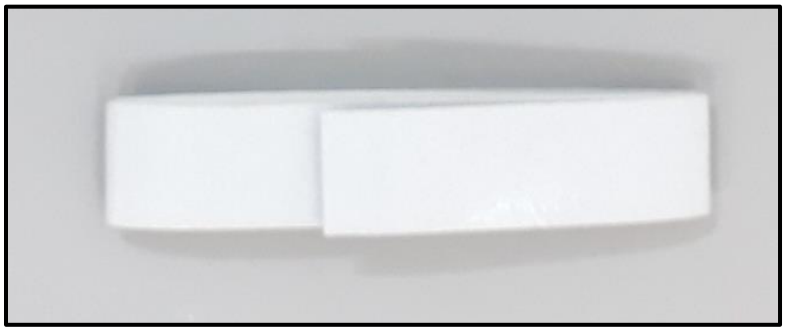

Figure 58. Reflective tape.

5.1.4 Cylindrical extension

The cylindrical extension is an accessory provided by the manufacturer of the water tunnel that we will use in order to achieve a directed and constant flow in which our propeller will be placed.

Figure 59. Cylindrical extension.

5.2 EXPERIMENTAL INSTALLATION

All tests were carried out in the fluid mechanics laboratory located in IPB-ESTIG, subsoil.

5.2.1 Flow calculation

In order to know the flow of the flow provided by our water tunnel, the calculations used in Souza [1] will be used, trusting that these are correct and were calculated with good judgment.

Next, we will explain how the procedure went.

1. Hose placement to direct the flow to a receiving vessel.
2. Using the help of a chronometer, measure the time in which X amount of water was deposited in the container.
3. Using the help of a balance, the weight of the extracted fluid will be calculated. For this, the container had to be previously weighed in TARA, and then the final weighing with the fluid obtained.
4. Already knowing the time, the mass of the fluid obtained and the specific mass of the water can be calculated the mass flow.

$$Q = \frac{(m_f - m_o)}{\rho . \Delta t} \qquad [47]$$

5. Fluid velocity is calculated

$$U = \frac{Q}{\pi . r_s^2} \qquad [48]$$

All the values used and obtained for the calculation of the flow are presented in the following table (Table 16), this was obtained as already mentioned from Souza's experimentation [1].

Table 16. Parameters for flow calculation.

Description	Symbol	Value
Initial mass of the container	m_i	1.45 kg
Final mass of the container	m_f	30.30 kg
Specific mass of water	ρ	999 kg/m^3
Timed time	Δt	8.36 s
Caudal	Q	0.0034 m^3/s
Section radius	r_s	0.0375 m
Fluid velocity	Or	0.78 m/s

5.3 EXPERIMENTAL PROCEDURES

The experimental work was carried out in different test sessions through the days, this was according to the availability of the laboratory and the logistics of the propellers delivered by the 3D printing department. To avoid any type of error, the same methodology was applied for each batch of tests, ensuring the comparability of these.

5.3.1 Positioning

The positioning of the propeller with the base and the orientation of the base within the hydraulic channel is one of the factors of greatest interference in the result of the measurement. This being in an incorrect positioning, either non-parallel with the flow or with some inclination will cause transverse forces to be generated in the axis of the propeller causing turbulence, deformations, etc.

Figure 60. positioning of the propeller.

5.3.2 Reading revolutions

The realization of the reading of the revolutions was carried out through different batches of rehearsals. Each propeller was tested in batches of between 1 to 2 minutes thus obtaining at least 50 RPM measurements in each one, this value obviously varied according to the rotational speed of each propeller.

The counting of the revolutions becomes effective once the state of regime of the hydraulic channel has been reached until the chosen arbitrary time has occurred (1 minute).

The number of batches varied, always trying to reach at least 250 measurements. With this in mind, at least 5 runs were achieved in each propeller, being that in some up to 7 runs were achieved thus generating the effectiveness of more than 400 RPM measurements.

The calculation of the optimal sample size was carried out through the formula that does not know the size of the population.

$$N_{opt} = \frac{Z^2 . p . q}{d^2} \quad [49]$$

- Z= confidence level.
- p= probability of success (expected proportion).
- Q= probability of failure.
- d^2= accuracy (maximum permissible error in terms of proportion).

We assume a security of 95% (0.95) which gives us a Z value of 1.65 according to Figure 61. Since we do not know the probability of success, the conservative criterion of p=q=0.5 has to be used. In this case, it seems reasonable to expect an accuracy of 5% taking into account the values presented by Souza [1].

α	Zα/2(2 colas)	β	Zβ(1 cola)
0.1	1.65	0.2	0.84
0.05	1.96	0.1	1.28
0.01	2.58	0.05	1.65

Figure 61. Frequent values.

Taking these values into account, the optimal sample size is calculated.

$$N_{opt} = 272$$

In this work, the value of at least 250 samples is arbitrarily adopted to achieve a well-marked trend of the rotational speed, a value close to the optimum, being judicious that this sampling value is sufficient.

The reading was made through the use of the aforementioned tachometer. For this, the reflective tape provided by the manufacturer of the tachometer was used, which was placed on the axis of each propeller. Once the channel has entered a state of regime, the optical reader is pointed at the reflective tape by holding down the read button constantly.

The tachometer must be positioned horizontally and fixed, since any disturbance of this can introduce a human error to the measurement, to avoid this, the tachometer was supported with the acrylic wall of the hydraulic channel trying to keep it immobile throughout the test.

Being a relatively old tachometer, its memory is not able to provide all the results obtained by reading during the time the button was pressed. The internal memory of the instrument only reports three results: The highest value, the lowest value and the last value obtained.

In order to memorize the readings, the filming was carried out directly from the tachometer screen and then manually inserted on an Excel file.

5.3.3 Water column reading

The second measurement achieved, to estimate the value of the power extracted by the turbines, is the difference in height of the water column. At first the water level is marked by the hydraulic channel in a stationary regime without the introduction of the propeller, this value will be the reference value to then calculate the difference that is generated with the introduction of the different propellers.

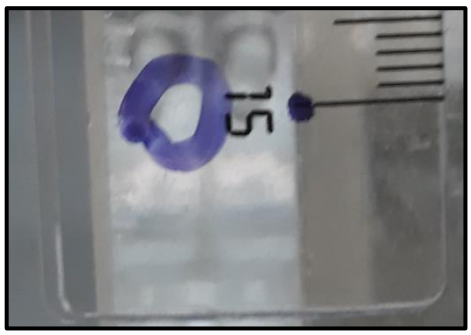

Figure 62. Value 0 of the water column.

The hydraulic power is obtained through the [50] , taking into account values of Table 16. In this case, we tried to avoid as much error as possible when measuring, since the surface tension of the water against acrylic is great and generates difficulty when measuring.

$$P_h = \rho . g . Q . \Delta h \quad [50]$$

5.4 LIMITATIONS

Souza [1] states that, due to the difficulties in regulating and reading the flow through the water tunnel, due to some damaged components, the experimental tests were carried out with the propeller inserted in the acrylic extension, where the value obtained experimentally for the fluid velocity in this section is 0.78 m/s, approximately 11% higher than estimated by the project. This value is considered acceptable and does not adversely influence the experimental comparison between the propellers, since the fluid velocity is the same for both. In addition, the short length of this extension does not allow the flow to fully develop, but for comparison purposes the propellers will be placed in the same position as recommended by the author.

As already mentioned above, the positioning of the propeller with respect to the flow is of vital importance. During the conduct of the experiments, it was possible to perceive the difficulty of achieving this, either by visualizing the axis to be flexed, the variability of the speed between batches where the positioning was minimal, or by means of a sudden braking of the axle during the test. This can be given by the following causes:

- a bearing already in poor condition which does not generate a free rotation and introduces high friction forces.
- Poor positioning of the bearing within the base cavity.
- A small mismatch of the base that generates difficulty when parallelizing the propeller.
- A high length of the axis that causes it to flex considerably.

Another important factor is the magnitude of the measures used in these trials. By reducing the parameter of the number of blades from 10 to 3, and being proportional to the length of the rope, very small lengths were achieved that make it difficult to carry out an experimentation in an accurate way. This can be modified by increasing the size of the propeller, which would cause a modification to be introduced into the diameter of the acrylic extension.

6. RESULTS

The results obtained during the laboratory test will be presented below. These consist of the angular velocity of each propeller and the difference in water column height.

For each propeller, a graph was made with the totality of the samples, also calculating and representing in horizontal lines the mean, the upper deviation and lower deviation for each one.

6.1 MEASUREMENT

As mentioned above, RPM measurements were made via a digital tachometer. Due to its memory characteristic, the measurements were video-recorded and then manually transported to an *EXCEL* spreadsheet.

6.1.1 Propeller 1

In reference to propeller 1, 237 measurements divided into 5 batches were read, thus presenting a graph like that of Figure 63 and Figure 64.

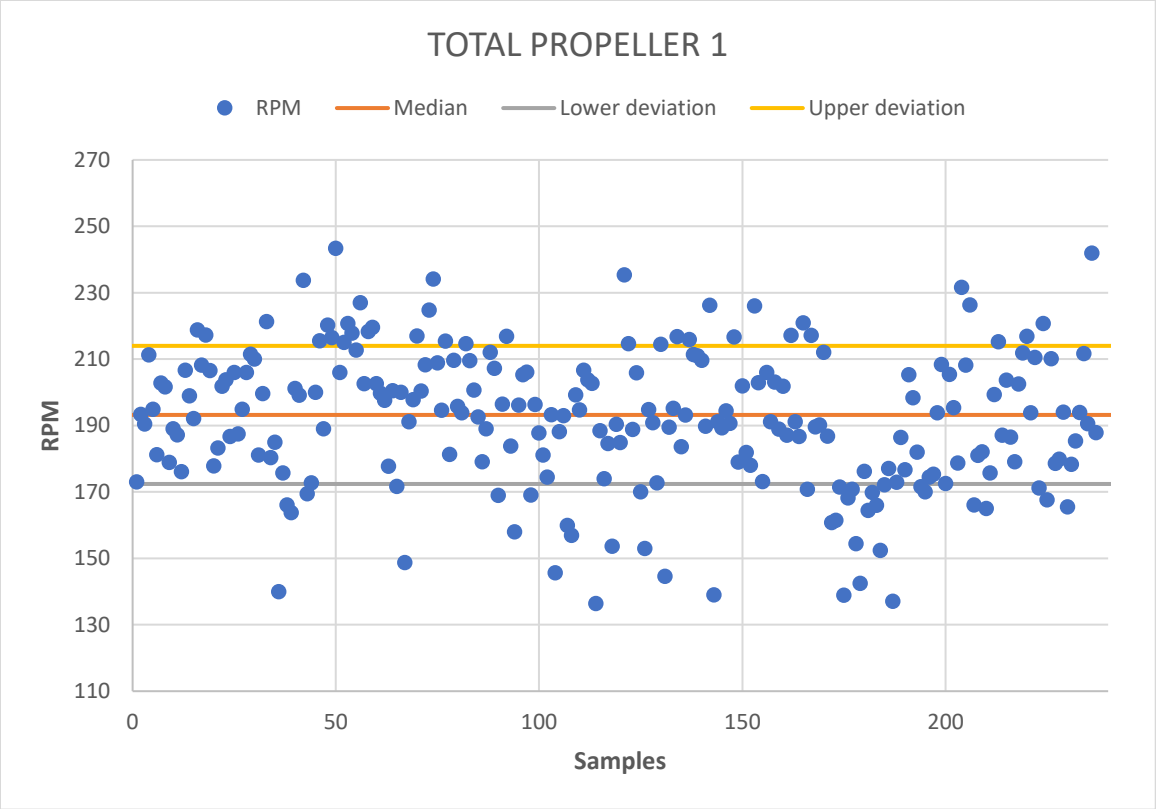

Figure 63. Propeller results 1.

Median	193,2
Deviation	20,79
Lower deviation	213,99
Upper deviation	172,41

Figure 64. RPM propeller 1.

The height of the water column was obtained through the difference obtained with the value 0. This was measured through a ruler on the acrylic wall.

$$\Delta h = 09\ mm$$

6.1.2 Propeller 2

In reference to propeller 2, 241 measurements divided into 5 batches were read, thus presenting a graph such as that of Figure 65 and Figure 66.

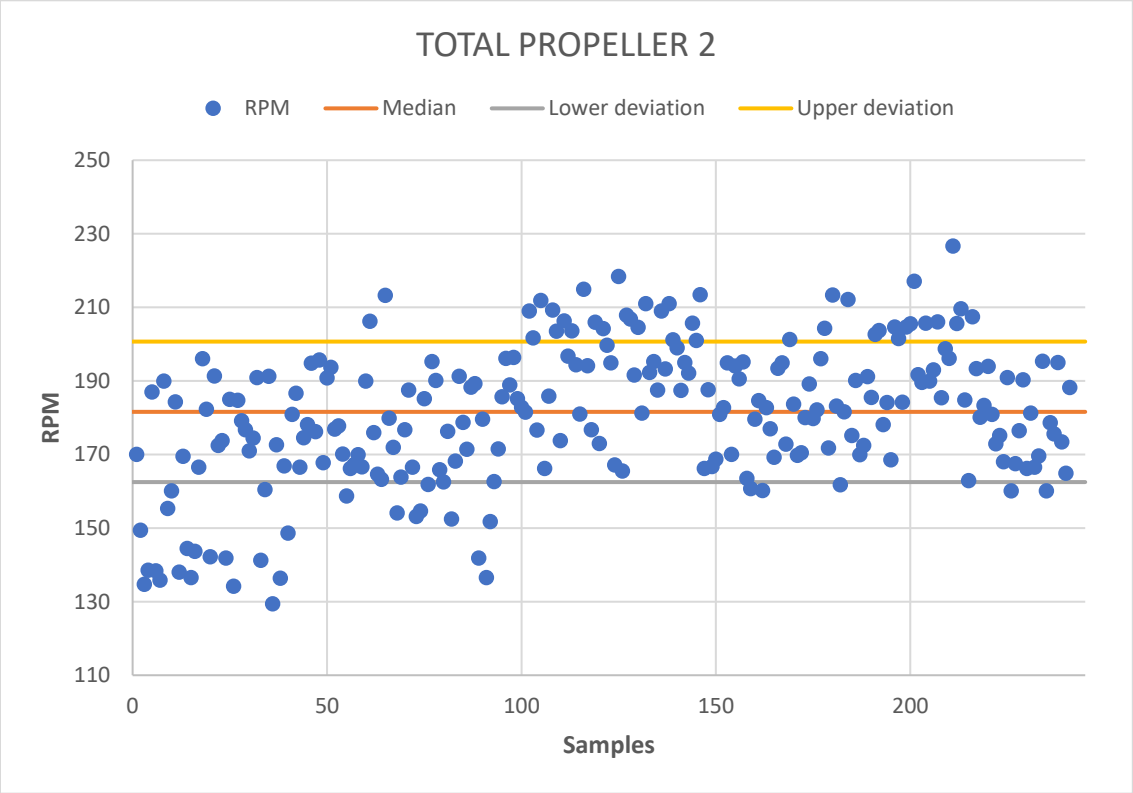

Figure 65. Propeller results 2.

Median	181,6
Deviation	19,10
Upper deviation	200,70
Lower deviation	162,50

Figure 66. RPM propeller 2.

The height of the water column was obtained through the difference obtained with the value 0. This was measured through a ruler on the acrylic wall.

$$\Delta h = 08\ mm$$

6.1.3 Propeller 3

In reference to propeller 3, 406 measurements divided into 7 batches were read, thus presenting a graph like that of Figure 67 and Figure 68.

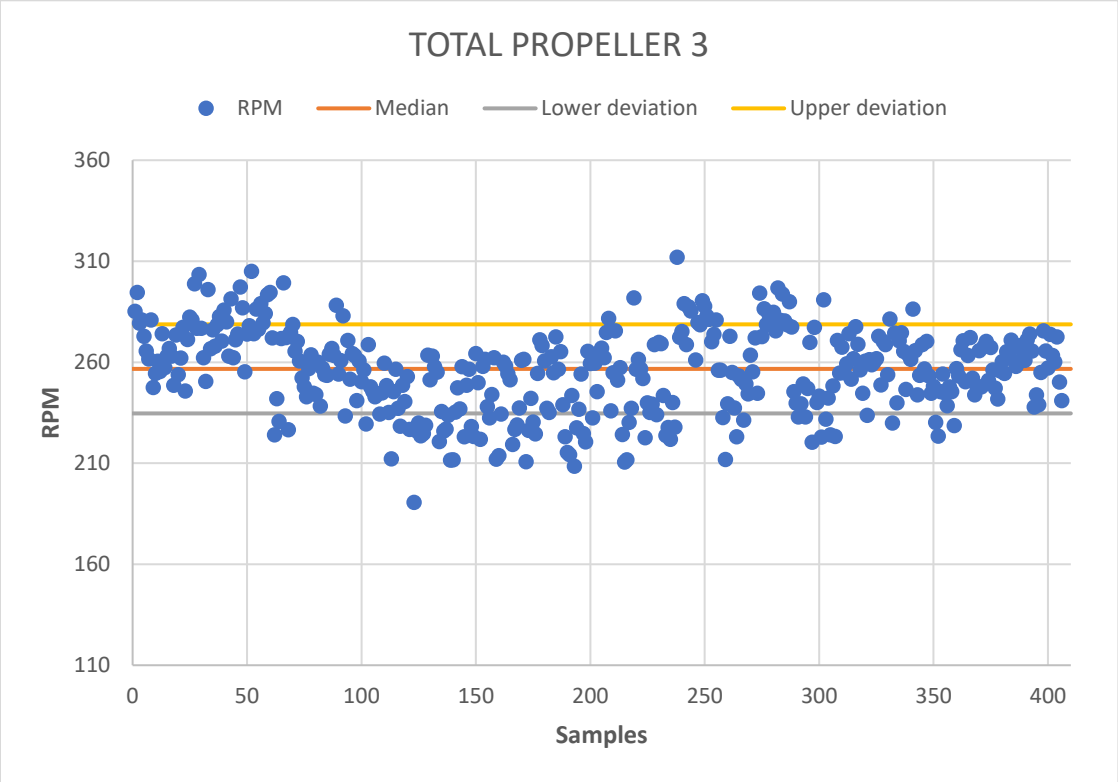

Figure 67. Propeller results 3.

Median	256,7
Deviation	22,04
Upper deviation	278,74
Lower deviation	234,66

Figure 68. RPM propeller 3.

The height of the water column was obtained through the difference obtained with the value 0. This was measured through a ruler on the acrylic wall.

$$\Delta h = 09\ mm$$

6.1.4 Propeller 4

In reference to propeller 4, 363 measurements divided into 6 batches were read, thus presenting a graph like that of Figure 69 and Figure 70.

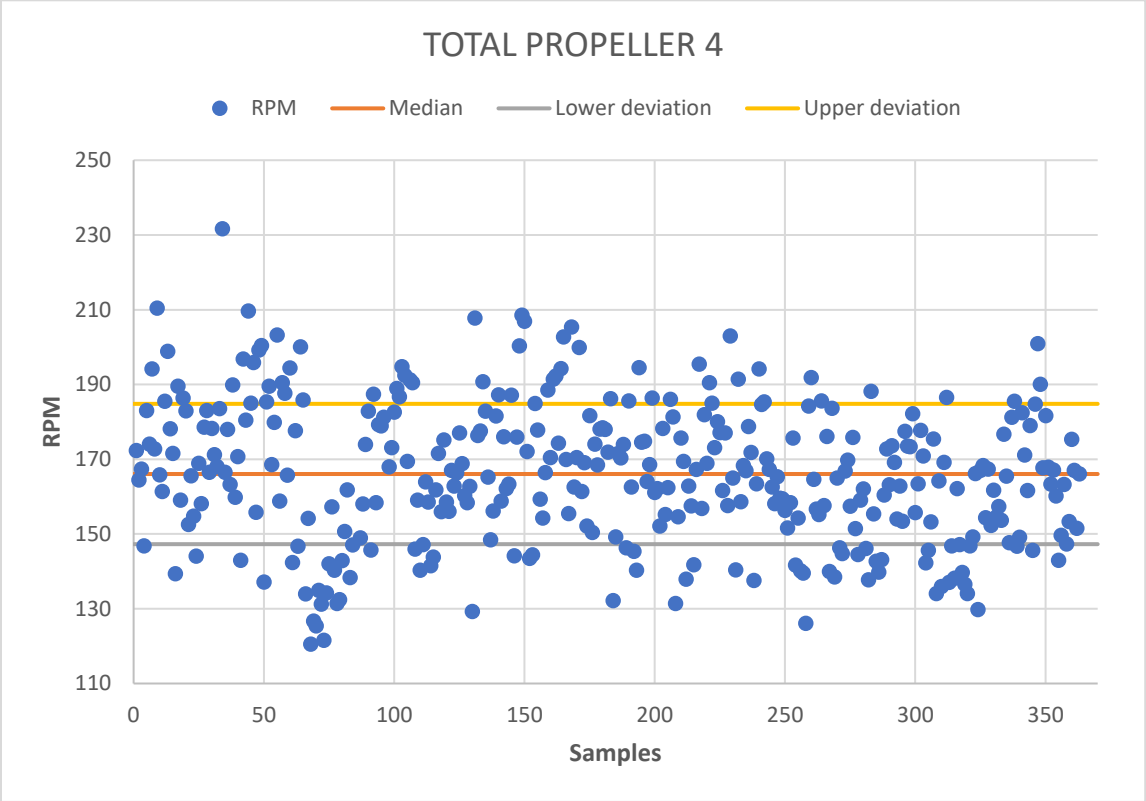

Figure 69. Propeller results 4.

Median	166,05
Deviation	18,77
Upper deviation	184,82
Lower Deviation	147,28

Figure 70. RPM propeller 4.

The height of the water column was obtained through the difference obtained with the value 0. This was measured through a ruler on the acrylic wall.

$$\Delta h = 09\ mm$$

6.1.5 Propeller 5

In reference to propeller 5, 259 measurements divided into 5 batches were read, thus presenting a graph like that of Figure 71 and Figure 72.

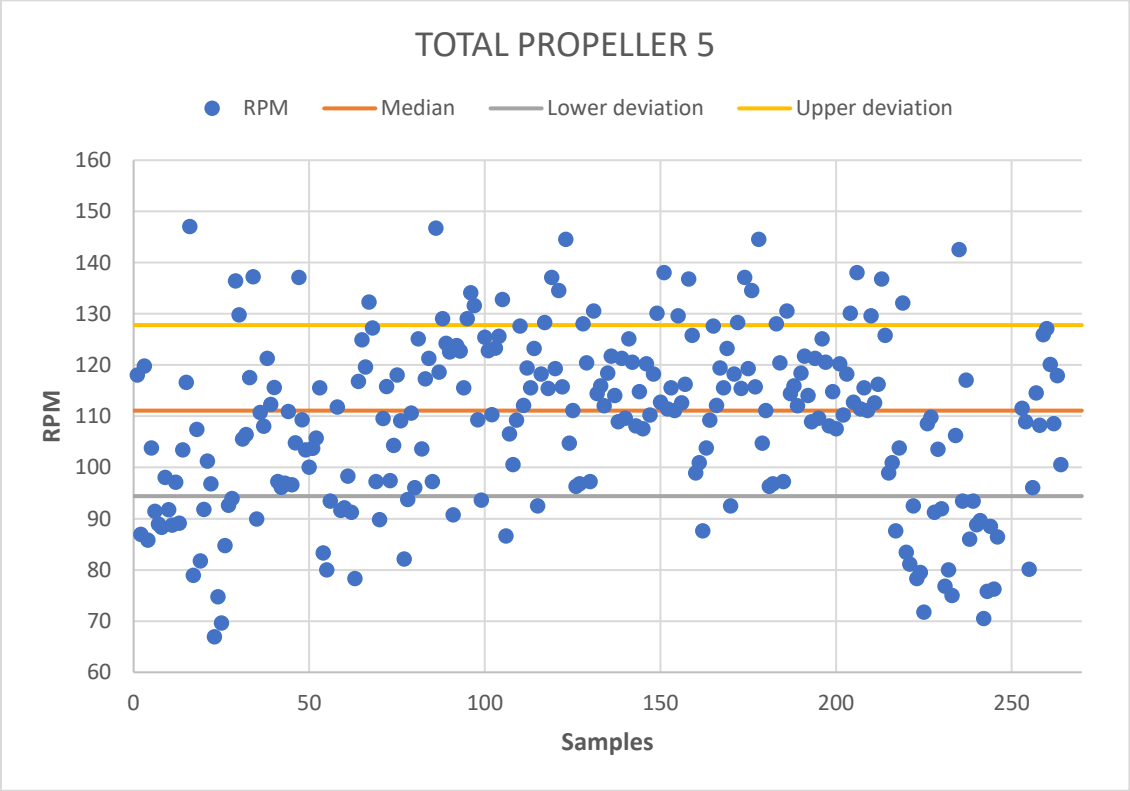

Figure 71. Propeller results 5.

Median	111,1
Deviation	16,70
Upper deviation	127,80
Lower deviation	94,40

Figure 72. RPM propeller 5.

The height of the water column was obtained through the difference obtained with the value 0. This was measured through a ruler on the acrylic wall.

$$\Delta h = 09\ mm$$

7. ANALYSIS OF THE RESULTS

In this chapter we will make a detailed analysis of the results with the intention of being able to obtain accurate conclusions and meet both **objective 5** and **objective 6**. First of all, we will start by making use of the graph obtained by Souza [1] where based on equation [46] sand graphed the curves of the power coefficients of propellers with different amounts of blades (B) depending on the ratio of tip speed λ considering the parameters of our project which are coincident with that of Souza's project [1].

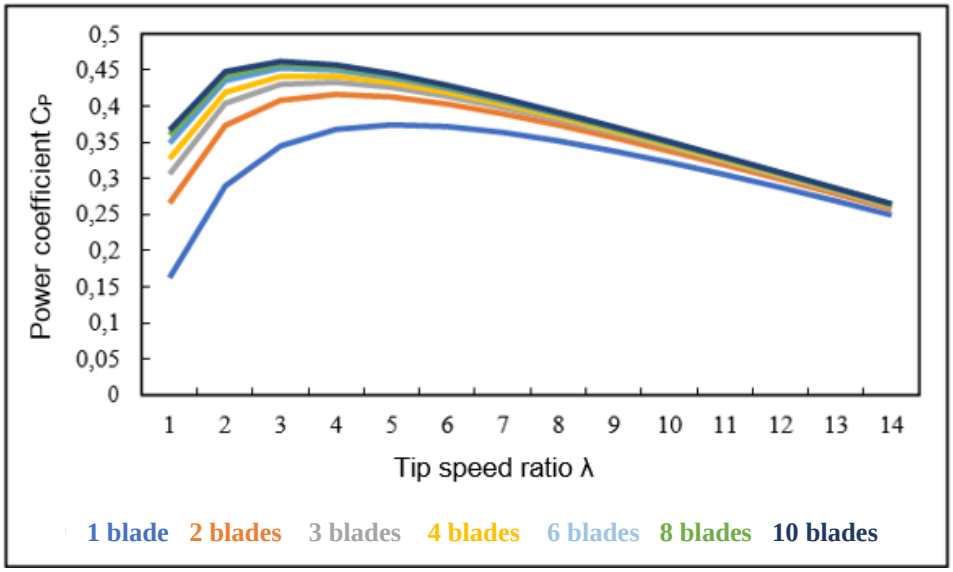

Figure 73. Power coefficient including all losses.

Taking into account this graph, and equation [46] we obtain the maximum possible value of the power coefficient C_p for a 3-blade propeller. C_p=0.425.

It is important to note, as already discussed in the limitations section, that there are differences between theoretical parameters and practical parameters. The propellers were designed to obtain the highest performance at a flow rate of 0.7 m/s, with the hydraulic channel generating a flow rate of 0.78 m/s, i.e., a difference of 11%.

By virtue of this percentage of the velocity increase, the available power will be altered considering that it is influenced by the velocity cube (U). Recalculating the available power (P_s) using equation [39] we obtain the new power available in practice, where:

- A: 0.001963 m^2.
- ρ: 999 kg/m^3.
- U: 0.78 m/s.

Being:

$$P_s = 0.4654\ watts$$

Knowing the available power (P_s) and the maximum power coefficient ($C_{p\ Max}$) we obtain the maximum power that we could obtain from a propeller of 3 blades through the product of these.

$$P_{Max} = 0.1978\ watts$$

The power extracted by the propellers is calculated based on the values obtained in the tests, i.e., the rotation reading (RPM) and the hydraulic power through the height differential measurement (Δh).

7.1.1 Propeller 1

Figure 63 and Figure 64. In short:

Table 17. Rpm and Δh propeller 1.

RPM	Δh (m)
193,2	0.009

Through equation [50] we can calculate the power extracted by the turbine using the difference in height of the water column (Δh), the volumetric flow (Q) and the hydraulic power of the same (P_h). From this we can also calculate the torque through equation (37) by dividing the extracted power by the rotational speed in [rad/s] and the power coefficient through equation (38).

- Hydraulic power
    - ρ = 999 [kg/m^3]
    - g = 9.81 [m/s^2]
    - Q = 0.0034 [m^3/s]

- Δh = 0.009 [m]

$$P_h = 0{,}2999\ Watts$$

- Torque

  - P_h = 0.2999 [Watts]
  - ω = 20.23 [rad/s]

$$T = 0{,}0148\ N.m$$

- Power coefficient

  - P = 0.2999 Watts.
  - P_s = 0.4654 Watts.

$$C_P = 0{,}64$$

Table 18. Propeller calculations 1.

Parameter	Symbol	Value
Hydraulic power	P_H	0,2999
Torque	T	0,0148
Power coefficient	C_P	0,64

7.1.2 Propeller 2

Figure 65 and Figure 66. In short:

Table 19. Rpm and Δh propeller 2.

RPM	Δh (m)
181,6	0,008

Through equation [50] we can calculate the power extracted by the turbine using the difference in height of the water column (Δh), the volumetric flow (Q) and the hydraulic power of

the same (P_h). From this we can also calculate the torque through equation (37) by dividing the extracted power by the rotational speed in [rad/s] and the power coefficient through equation (38).

- Hydraulic power

  - $\rho = 999$ [kg/m^3]
  - $g = 9.81$ [m/s^2]
  - $Q = 0.0034$ [m^3/s]
  - $\Delta h = 0.008$ [m]

$$P_h = 0{,}2665\ Watts$$

- Torque

  - $P_h = 0.2665$ [Watts]
  - $\Omega = 19.02$ [rad/s]

$$T = 0{,}0140\ N.m$$

- Power coefficient

  - $P = 0.2665$ Watts.
  - $P_s = 0.4654$ Watts.

$$C_P = 0{,}57$$

Table 20. Propeller calculations 2.

Parameter	Symbol	Value
Hydraulic power	P_H	0,2665
Torque	T	0,0140
Power coefficient	C_P	0,57

7.1.3 Propeller 3

Figure 67 and Figure 68. In short:

Table 21. Rpm and Δh propeller 3.

RPM	Δh (m)
256,7	0,009

Through equation [50] we can calculate the power extracted by the turbine using the difference in height of the water column (Δh), the volumetric flow (Q) and the hydraulic power of the same (P_h). From this we can also calculate the torque through equation (37) by dividing the extracted power by the rotational speed in [rad/s] and the power coefficient through equation (38).

- Hydraulic power

  - ρ = 999 [kg/m^3]
  - g = 9.81 [m/s^2]
  - Q = 0.0034 [m^3/s]
  - Δh = 0.009 [m]

$$P_h = 0{,}2999\ Watts$$

- Torque

  - P_h = 0.2999 [Watts]
  - ω = 26.88 [rad/s]

$$T = 0{,}0111\ N.m$$

- Power coefficient

  - P = 0.2999 Watts.
  - P_s = 0.4654 Watts.

$$C_P = 0{,}64$$

Table 22. Propeller calculations 3.

Parameter	Symbol	Value
Hydraulic power	P_H	0,2999
Torque	T	0,0111
Power coefficient	C_P	0,64

7.1.4 Propeller 4

The experimental results of propeller 1 are shown in Figure 69 and Figure 70 . In short:

Table 23. Rpm and Δh propeller 4.

RPM	Δh (m)
166,05	0,009

Through equation [50] we can calculate the power extracted by the turbine using the difference in height of the water column (Δh), the volumetric flow (Q) and the hydraulic power of the same (P_h). From this we can also calculate the torque through equation (37) by dividing the extracted power by the rotational speed in [rad/s] and the power coefficient through equation (38).

- Hydraulic power
    - ρ = 999 [kg/m^3]
    - g = 9.81 [m/s^2]
    - Q = 0.0034 [m^3/s]
    - Δh = 0.009 [m]

$$P_h = 0{,}2999\ Watts$$

- Torque
    - P_h = 0.2999 [Watts]
    - ω = 17.38 [rad/s]

$$T = 0{,}0173\ N.m$$

- Power coefficient

  - P = 0.2999 Watts.
  - P_s = 0.4654 Watts.

$$C_P = 0{,}64$$

Table 24. Propeller calculations 4.

Parameter	Symbol	Value
Hydraulic power	P_H	0,3332
Torque	T	0,0173
Power coefficient	C_P	0,64

7.1.5 Propeller 5

Figure 71 and Figure 72. In short:

Table 25. Rpm and Δh propeller 5.

RPM	Δh (m)
111,1	0,009

Through equation [50] we can calculate the power extracted by the turbine using the difference in height of the water column (Δh), the volumetric flow (Q) and the hydraulic power of the same (P_h). From this we can also calculate the torque through equation (37) by dividing the extracted power by the rotational speed in [rad/s] and the power coefficient through equation (38).

- Hydraulic power

  - ρ = 999 kg/m^3

- g = 9.81 m/s^2
- Q = 0.0034 m^3/s
- Δh = 0.009 m

$$P_h = \ 0{,}2999\ Watts$$

- Torque

- P_h = 0.2999 [Watts]
- ω = 11.63 [rad/s]

$$T = 0{,}0257\ N.m$$

- Power coefficient

- P = 0.2999 Watts.
- P_s = 0.4654 Watts.

$$C_P = 0{,}64$$

Table 26. Propeller calculations 5.

Parameter	Symbol	Value
Hydraulic power	P_H	0,2999
Torque	T	0,0257
Power coefficient	C_P	0,64

8. CONCLUSION

In the present work, the experimentation of 5 propellers with different construction parameters was carried out with the motivation of studying their results and better understanding their operation / performance in the face of the growing demand for mini-hydroelectric turbines in riverbeds. These were developed through the iterative method capable of calculating the elements of the propeller blade with the aim of improving its performance. In this method we use null interference values, which, for a first experimentation is acceptable considering that it will introduce performance losses.

With respect to **objective 5**, Table 3 indicates the practically recommended tip speed ratio (λ) in relation to the number of propeller blades (B). This indicates that to obtain propellers of greater performance, the number of tip speed ratio (λ) must be increased as we decrease the number of blades (B). The propellers experienced demonstrate a behavior in accordance with that predicted by Table 3, where having equal extracted power values for propellers 3, 4 and 5 results in greater torque as λ increases. That is, propeller 4 generates more torque than propeller 3 and propeller 5 of propeller 4.

With respect to the power coefficients obtained (C_p), these have values greater than the Betz power coefficient ($C_{P\ ideal} = 0.593$) that is, we are obtaining power values greater than the limits indicated by the theory. This can be explained either because, the power supplied (P_s) is not correct, and the water channel delivers a higher power or an erroneous measurement of the parameter Δh.

The supplied power coefficient (P_s) can take an incorrect value due to an incorrect flow rate value (U), i.e., the speed we obtained from the flow rate (Q) is less than the real one.

On the other hand, the hydraulic power (P_h) can take an incorrect value due to 2 values, firstly, an erroneous flow value (Q) that would be compensated with the parameter U present in the P_s, therefore, this possibility is ruled out. Leaving as the only option the value of Δh which introduces an error at the time of measurement due to the difficulty of making the reading when the water channel is in operation either by the generation of vibrations added to the error by the

surface tension of the water in contact with the acrylic wall, that it is step said, it is of a considerable thickness which makes it difficult with a majority to measure this value.

With respect to **objective 6**, there is a decrease in the rotation speed of the "optimized" propeller compared to the "non-optimized" propeller designed by the Souza parameters [1], therefore, a decrease in the power, torque and C_p obtained, which goes against what was sought with respect to the introduction of interference factors in the design of the propeller. This demonstrates the importance of designing a propeller taking into account the number of blades that it will have from the beginning, and the error that would entail designing a universal blade and then conferring propellers of different values of number of blades.

Finally, in future experiments, recommend the introduction of interference factors in propeller 3, propeller 4 and propeller 5. Once these factors are obtained, compare them with each other and verify if the expected condition is met.

Increasing the rotor diameter will be a beneficial change for research, as it will allow experimenting with smaller λ propeller designs thus broadening the spectrum of experimentation. On the other hand, it would be interesting to study the behavior with propellers of greater robustness. The introduction of dimensionless numbers such as Euler, Mach, Weber, etc. They would be an interesting factor to analyze.

Base improvement is a crucial process, as experimentation is significantly affected by propeller positioning, bearing quality, and forces unwrapped by the propeller's parallelism with flow. The design of a basis that allows experimentation to be systematically reproduced without changing conditions will be an important step in this chain of research. Likewise, as the decrease in the length of the shaft of the propeller that will allow us to reduce harmful bends for the rotation of this.

Finally, the arrangement of the flow meter of the water channel would be important to obtain real and instantaneous values of the flow that the propeller will be using taking into account that in slightly old machinery this can be inconsistent.

9. REFERENCES

[1] Souza, T. (2020). Otimização experimental de miniturbina hidráulica. Instituto politecnico Braganza. CEFET.

[2] Plana, C. M. (2009). Turbomáquinas hidráulicas: turbinas hidráulicas, bombas, ventiladores (Vol. 2). Universidad Pontificia Comillas.

[3] Díez, P. F. (1996). Turbinas hidráulicas. Departamento de Ingenieria Electrica y Energética. Universidade de Cantabria, Espanha,

[4] Quispe, F. M. (2005). Diseño de una turbina de río para la generación de electricidad en el distrito de Mazán-Región Loreto. Universidad nacional mayor de San Marcos

[5] NAVA MASTACHE. (2013) Arturo. Selección y dimensionamiento de turbinas hidráulicas para centrales hidroeléctricas. Universidad Nacional Autónoma de México.

[6] Teresa Reyna, María Lábaqueb, Santiago Reynac, César Rihad, Belén Irazusta. (2018) Energía mini y micro hidráulica: aporte contra el Cambio Climático. Universidad Nacional de Córdoba

[7] TURBINAS KAPLAN (2022) componentes, eficiencia y aplicaciones. (s/f). Tecnologypoint.com. https://www.tecnologypoint.com/turbinas-kaplan/

[8] Energía Hidráulica. (2019). Proyecto Transición Energética. https://transicionenergetica.do/sobre-nosotros/energia-hidraulica/

[9] Mini Central Hidroeléctrica de Condor. (2022). Quadrante-engenharia.pt. https://www.quadrante-engenharia.pt/es/proyectos/water-utilities/mini-central-hidroelectrica-de-condor/

[10] JANSEN, Wim AM; SMULDERS, Paul Thomas. (1977) Rotor design for horizontal axis windmills. SWD publications, v. 7701.

[11] JUNIOR, Miguel Luís Belmonte. (2017) Otimização da geometria de pás para turbina eólica de eixo horizontal. Trabalho de Conclusão de Curso.

[12] WENZEL, Guilherme München. (2007) Projeto aerodinâmico de pás de turbinas eólicas de eixo horizontal. Revista da Graduação, v. 1, n. 10

[13] FERNANDES, Rui F.C. (2017) Estudo, desenvolvimento e concessão de militurbinas hidráulicas com o recurso de impressoras 3D. Dissertação de Mestrado. Universidade do Minho, Portugal.

[14] Material de filamento Ultimaker PLA para impresora 3D: altamente versátil y fácil de imprimir | Ultimaker

[15] Hydraulic Channels — ELD (eldinc.com)

[16] Cálculo del tamaño óptimo de una muestra (ucc.edu.co)

[17] Cálculo del tamaño de la muestra en investigación en educación médica | Investigación en Educación Médica (elsevier.es)